



## OPEN ACCESS

## EDITED BY

Eleonora Puccinelli,  
Université Bretagne Occidentale,  
France

## REVIEWED BY

Dong Feng,  
Shanghai Ocean University, China  
Crispin Thomas Stephen Little,  
University of Leeds, United Kingdom

## \*CORRESPONDENCE

Emmelie K. L. Åström  
emmelie.astrom@gmail.com

## SPECIALTY SECTION

This article was submitted to  
Deep-Sea Environments and Ecology,  
a section of the journal  
Frontiers in Marine Science

RECEIVED 01 April 2022

ACCEPTED 18 July 2022

PUBLISHED 17 August 2022

## CITATION

Åström EKL, Bluhm BA and  
Rasmussen TL (2022) Chemosynthetic  
and photosynthetic trophic support  
from cold seeps in Arctic benthic  
communities.  
*Front. Mar. Sci.* 9:910558.  
doi: 10.3389/fmars.2022.910558

## COPYRIGHT

© 2022 Åström, Bluhm and Rasmussen.  
This is an open-access article  
distributed under the terms of the  
[Creative Commons Attribution License  
\(CC BY\)](https://creativecommons.org/licenses/by/4.0/). The use, distribution or  
reproduction in other forums is  
permitted, provided the original  
author(s) and the copyright owner(s)  
are credited and that the original  
publication in this journal is cited, in  
accordance with accepted academic  
practice. No use, distribution or  
reproduction is permitted which  
does not comply with these terms.

# Chemosynthetic and photosynthetic trophic support from cold seeps in Arctic benthic communities

Emmelie K. L. Åström<sup>1\*</sup>, Bodil A. Bluhm<sup>1</sup>  
and Tine L. Rasmussen<sup>2</sup>

<sup>1</sup>Department of Arctic and Marine Biology, UiT-The Arctic University of Norway, Tromsø, Norway,

<sup>2</sup>CAGE, Centre for Arctic Gas Hydrate, Environment and Climate, Department of Geosciences, UiT-The Arctic University of Norway, Tromsø, Norway

Benthic communities below the photic zone are largely reliant on the export of surface-water primary production and the flux of partially degraded organic matter to the seabed, i.e. pelagic–benthic coupling. Over the past decades, however, the role of chemosynthetically produced carbon in food webs has been recognized in various habitats. Cold seeps are now known to be widespread across circumpolar Arctic shelves where natural release of hydrocarbons occurs at the seabed. Here, we investigated to what extent chemosynthesis-based carbon (CBC) enters the food web in a high latitude shelf-system. Specifically, we estimated the contributions of chemosynthesis-based carbon to primarily benthic invertebrate taxa from seeps at both shallow and deeper shelves and comparative non-seep areas in the Svalbard–Barents Sea region using bulk stable isotope-analysis of carbon and nitrogen. Our results show low  $\delta^{13}\text{C}$  values ( $-51.3$  to  $-32.7$ ‰) in chemosymbiotic siboglinids and several species of benthic, higher-trophic level, invertebrates (mainly polychaetes and echinoderms;  $-35.0$  to  $-26.1$ ‰) collected at cold seeps, consistent with assimilation of chemosynthesis-based carbon into the Arctic benthic food web. Using a two-component mixing equation, we demonstrate that certain species could derive more than 50% of their carbon from chemosynthesis-based carbon. These findings show that autochthonous chemosynthetic energy sources can contribute to supporting distinct groups of ‘background’ benthic taxa at these Arctic seep-habitats beyond microbial associations and chemosymbiotic species. Furthermore, we found a higher degree of chemosynthesis-based carbon in benthos at the deeper Barents Sea shelf seeps ( $>330$  m) compared to seeps at the Western Svalbard shelf ( $<150$  m water-depth), and we suggest this result reflects the differences in depth range, surface production and pelagic–benthic coupling. We detected large intra-species variations in carbon signatures within and across geographical locations and, combined with isotopic niche-analysis, our results show that certain taxa that inhabits seeps, have wider trophic niches in comparison to taxa inhabiting non-seeps. The increasing number of discovered natural seeps in the Arctic suggests that chemosynthetic production from seeps could play a more critical role in Arctic trophic structure than previously thought.

Seep-derived carbon should, hence, be accounted for as an additional carbon source and included in food-web and energy-flow models in future work.

#### KEYWORDS

methane, chemosynthesis, food web, benthos, Svalbard

## Introduction

Large-scale spatial and seasonal variations in marine primary production combined with water-depth gradients and vertical transport of particulate organic matter largely regulate the composition and function of benthic communities (Ambrose and Renaud, 1995; Wassmann et al., 2006). Heterotrophic benthic communities are dependent on an export of surface-water photosynthetic production to the seafloor at depths below the euphotic zone and beyond the coasts (i.e. pelagic-benthic coupling) (Graf, 1989; Grebmeier and Barry, 1991; Wiedmann et al., 2020). Depending on latitude, surface primary production is strongly linked to seasonal environmental cycles and, in the high-Arctic, primary production occurs during an intense growth period and short time-interval. In addition to the surface-water phytoplankton production, sea-ice algae are an important photosynthetic carbon source in Arctic ice-covered waters, especially in the early growth season (Syvertsen, 1991; Hegseth and Quillfeldt, 2022). Ice-algae can contribute to large algae-falls to benthic systems (Boetius et al., 2013). The view of vertical transport of carbon sources to seafloor communities, however, is based on carbon originating solely from photosynthesis and produced in ocean surface-waters. Conversely, at cold seeps, where hydrocarbons such as methane emanate from the seafloor, chemosynthesis can serve as an alternative energy source to photosynthesis (Childress et al., 1986; Levin and Michener, 2002; Boetius and Suess, 2004). The coupled anaerobic oxidation of methane (AOM) and sulphate reduction in the sediment by microbial consortia allow organisms to utilize hydrocarbon sources directly *via* chemosynthesis and symbiotic associations with methanotrophs or thiotrophs, or indirectly *via* trophic predator-prey interactions (Boetius and Suess, 2004; Decker and Olu, 2012; Higgs et al., 2016). These symbiotic relationships and trophic interactions can result in unique habitats consisting of specialized chemosymbiotic faunal communities and associated macrofauna (Childress et al., 1986; Levin et al., 2016).

Carbon acquires specific isotopic values depending on the carbon fixation pathways and it produces a distinct imprint of the surrounding environment. Combining the analyses of stable isotope ratios of carbon ( $\delta^{13}\text{C}$ ) and nitrogen ( $\delta^{15}\text{N}$ ) to

assess the nature of carbon sources and the trophic structure, it is possible to document ecosystem characteristics and predator-prey interactions, and generate insight on resource utilization (Childress et al., 1986; Zanden and Rasmussen, 2001; Post, 2002). Carbon assimilated through chemosynthesis can get, *via* Rubisco I catalyst in the Calvin Benson Bassam Cycle, distinct  $^{13}\text{C}$ -depleted values, typically  $\delta^{13}\text{C} < -30\text{‰}$  (Robinson and Cavanaugh, 1995; Hügler and Sievert, 2011) compared to photosynthesized organic carbon ( $\delta^{13}\text{C}$  typically  $\sim -25\text{‰}$  to  $-20\text{‰}$ ) and used as a tracer in marine food webs (Childress et al., 1986; Levin and Michener, 2002). The energetic pathway of chemosynthesis to marine organisms has been documented from cold seeps globally (Levin and Michener, 2002; Niemann et al., 2013; Zapata-Hernández et al., 2014). In deep-sea seeps, carbon produced *via* chemosynthesis is seen to be highly integrated in marine benthos, contributing to food resources and specialization of organisms (Levin et al., 2016; Toone and Washburn, 2020; Feng et al., 2021). The integration of chemosynthetic carbon in shallow cold-seep habitats, however, is not as apparent as for deep-sea systems and it is assumed that photosynthetic resources and vertical transport of organic matter play a more important role in shallow chemosynthetic-based systems (Tarasov et al., 2005; Stevens et al., 2015).

Cold seeps have been discovered in all world oceans, including the polar regions (Domack et al., 2005; Decker and Olu, 2012). In the Arctic, a common feature at seeps is the high degree of so called 'background fauna' and the absence of large chemosymbiotic species and specialized taxa beyond small siboglinids (Åström et al., 2016; Sen et al., 2019; Vedenin et al., 2020). Even though there are several descriptions of habitat characteristics and species composition, the knowledge of trophic structure and chemosynthesis-based carbon at Arctic seeps is inadequate, as are its pathways to ambient fauna. This gap in knowledge stands in contrast to other carbon sources that nowadays are recognized to contribute to benthic communities and marine Arctic food webs (Wiedmann et al., 2020). Several studies have focused on the input of photosynthetic sources including phytoplankton and ice algae (McMahon et al., 2006; Søreide et al., 2006) and in recent times, there has been an increased attention to examine the potential contribution of other carbon sources such as food falls (Dunlop et al., 2018), and

terrestrial and riverine organic matter (Bell et al., 2016; McGovern et al., 2020).

The Barents Sea region is considered a hotspot of marine productivity (Wassmann et al., 2006), and supports one of the world's most important commercial fisheries (Kjesbu et al., 2014). This region is also exposed to large-scale environmental changes because of rising temperatures (Fossheim et al., 2015) and is predicted to undergo extensive and concomitant changes in ocean circulation and reductions in sea ice (Onarheim and Årthun, 2017). These physical and oceanographical changes are expected to drive large-scale shifts in carbon cycling, trophic interactions and biological productivity (Wassmann et al., 2020; Ingvaldsen et al., 2021). To date, food web interactions at Arctic cold seeps have mainly been studied at the Håkon Mosby mud volcano (located at 1200 m water-depth at the Norwegian continental margin) (Gebruk et al., 2003; Decker and Olu, 2012; Georgieva et al., 2015). Here, chemosymbiotic fauna (two species of siboglinids *Sclerolinum contortum* and *Oligobrachia cf. haakonmosbiensis*) and microbial mats form a base for further trophic interactions with benthic organisms. As examples, depleted  $^{13}\text{C}$  values (-49 to -45‰) were recorded in gastropods, sea spiders, and a few polychaetes associated with microbial mats (Decker and Olu, 2012). In adjacent sediment, zoarcid fishes also showed  $^{13}\text{C}$  depleted values (-52 to -49‰) (Gebruk et al., 2003; Decker and Olu, 2012) and Gebruk et al. (2003) suggested that the zoarcids possibly had preyed on siboglinid polychaetes to acquire such low  $\delta^{13}\text{C}$  values. The high occurrence of natural methane seep sites at the circumpolar Arctic shelves and margins (Stranne et al., 2016; Shakhova et al., 2019) constitutes a potential carbon source for organisms inhabiting or passing through such habitats. However, to what extent such carbon source is exploited beyond the microbial communities is poorly investigated yet may provide critical information in food web and energy flow models that contribute to resource management.

Our aim with this study was, therefore, to quantify the potential use of chemosynthesis-based carbon from cold seeps to the general macro-benthic faunal community in a productive Arctic shelf in the south-west Barents Sea. We used stable isotope analyses of nitrogen and carbon of organism and known food-web baselines in the investigated systems to test the hypothesis that chemosynthesis-based carbon is used as a carbon source for a variety of non-chemosymbiotic taxa of the faunal community at seeps. Furthermore, we tested if the incorporation of chemosynthesis-based carbon differed between organisms sampled at shallow seeps (<150 m deep) and deeper seeps (>330–400m), including a recently discovered seep-site north of Svalbard. At the shallow seeps, we hypothesize that the influence of chemosynthesis-based carbon to the seep-community is diminished because of high photosynthetic primary-production and strong benthic-pelagic coupling.

## Material and methods

### Study area

Marine environments in the high-Arctic are characterized by intense seasonality of light, sea-ice cover, temperature, and productivity. At the continental margin of Svalbard and in the Barents Sea, the interaction and mixing of cold Arctic and warm Atlantic water-masses creates a productive shelf ecosystem with strong coupling of pelagic and benthic processes (Loeng, 1991; Wassmann et al., 2006). The climate in Svalbard and northwestern Barents Sea is relatively mild compared to other regions in the high-Arctic. This area is strongly affected by the West Spitsbergen Current and the transport of warm and saline Atlantic Water northwards into the Arctic Ocean (Figure 1). The western Svalbard margin consists of a shallow (<200 m) shelf off the island of Prins Karls Forland. The Barents Sea, a marginal sea to the Arctic Ocean is a shelf-sea with an average water-depth of approximately 230 m and the bathymetry is characterized by shallow banks and deeper troughs. The Barents Sea shelf is influenced by both warm and saline Atlantic water from southwest and cold Arctic water-masses from northeast, flowing in from the Arctic Ocean (Figure 1). The oceanic boundary of the polar front is formed where these two water-masses meet (Loeng, 1991). Along the western Svalbard margin and in the Barents Sea troughs, several natural hydrocarbon seeps occur near the predicted upper depth limit of the gas hydrate stability-zone, and where sub-seabed gas reservoirs release methane (Sahling et al., 2014; Mau et al., 2017). The targeted cold seep-locations in this study have all been covered by the Barents Sea Ice Sheet during the last glacial maximum. Present-day hydrocarbon emissions at the Svalbard shelf and margin is likely a result from dissolution of gas hydrate reservoirs in the sub-seabed caused by post-glacial isostatic rebound and sub-seabed migration of gas through faults and fracture zones (Portnov et al., 2016; Serov et al., 2017). At the western shelf and slope of Svalbard, extensive gas emission and elevated concentrations of methane in the water-column are reported in water-depths ranging from ~ 80–400 m (e.g. Sahling et al., 2014; Pohlman et al., 2017). In this study, we refer to this area as the Western Svalbard and Prins Karls Forland seeps (Figure 1, Table 1). In the western Barents Sea, south of Svalbard, two locations have been identified in the outer part of Storfjordrenna with sub-surface gas deposits and hydrocarbon seepage (Figure 1) referred to in this study as Storfjordrenna seeps and Gas Hydrate Mounds. Further east, an area of gas-seeping crater-mound complexes exist in the central Barents Sea at the rim of Bjørnøyrenna (Bear Island Trough) (Solheim and Elverhøi, 1993) (Figure 1, Table 1). See summarized descriptions of these study sites in Åström et al. (2020).

A previously undescribed seep area was found in the northern Svalbard area, north of the Hinlopen Strait

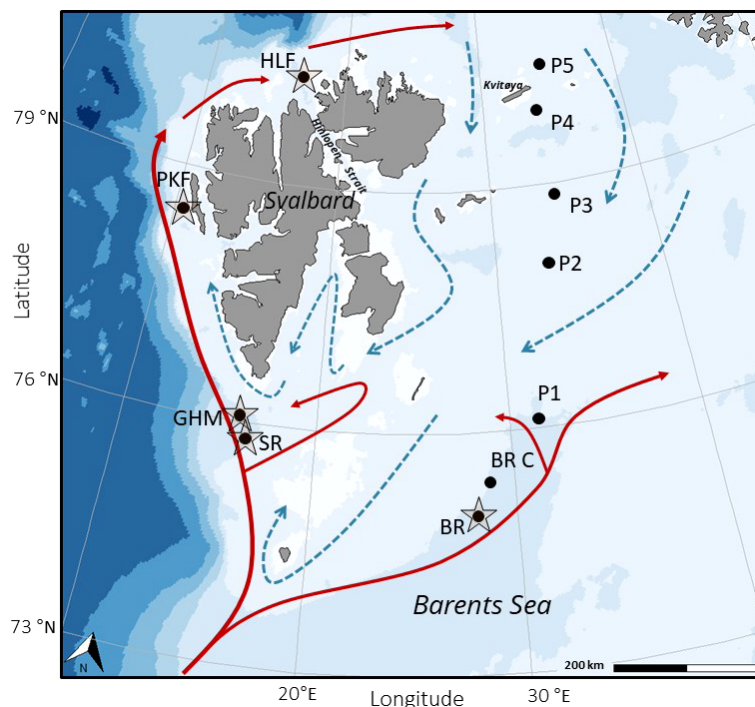


**FIGURE 1**  
Svalbard-Barents Sea study area with sampling locations. Arrows show overriding surface currents; Atlantic water mass (solid/red) and Arctic water mass (dashed/blue) (modified from (Loeng, 1991)). Sampling locations are marked as black circles, and stations at cold seeps are indicated by a star. For more information about sampling locations, see Table 1. Map was produced using package ggOceanMaps in R (Vihtakari, 2021).

**TABLE 1** Areas where samples and organisms for stable isotope analyses in this study have been collected.

Area	Station	Characteristics	Latitude N	Longitude E	Salinity (psu)	T (°C)	Depth (m)
Bjørnøyrenna	BR C	Non-seep	75°09'	28°35'	35.1	1.4	334
Bjørnøyrenna Crater field	BR	Seep	74°54'	27°33'	35.1	1.7	337
Central Barents Sea	P1	Non-seep	75°60'	31°13'	35.0	1.3	325
Central Barents Sea	P2	Non-seep	77°50'	34°00'	34.9	0.8	190
Central Barents Sea	P3	Non-seep	78°75'	34°00'	34.9	0.8	305
Northern Barents Sea	P4	Non-seep	79°45'	33°59'	34.8	-0.2	334
Northern Barents Sea	P5	Non-seep	80°50'	34°00'	34.6	-0.2	163
Hinlopen North	HLF	Seep	80°29'	16°10'	35.0	3.5	339
Prins Karls Forland	PKF C	Shallow Seeps	78°33'	10°10'	35.1	3.8	85-157
Prins Karls Forland	PKF	Non-seep	78°34'	10°09'	35.1	1.4	88
Storfjordrenna	GHM C	Non-seep	76°05'	15°58'	35.0	2.4	385
Storfjordrenna	SR C	Non-seep	75°52'	16°39'	35.1	2.4	350
Storfjordrenna Gas Hydrate Mounds	GHM	Seep	76°06'	16°00'	34.9	2.0	383
Storfjordrenna seep field	SR 1	Seep	75°50'	16°35'	35.1	2.4	353

Temperature (T) and salinity is given for bottom water.

(Figure 1). Here, relatively warm, saline water of Atlantic origin is transported southwards through the strait and cold Arctic water flows northwards (Figure 1) (Loeng, 1991). At the outer part of Hinlopen Strait, geophysical investigations and sediment analyses indicate thermogenic sources of methane in the seabed

(Blumenberg et al., 2016), where these authors suggest that methane and possibly heavier hydrocarbons stems from deeper source rocks and ice-rafted organic matter from nearby locations. Furthermore, geophysical investigations by Geissler et al. (2016) recorded clusters of acoustic flares in an area south

of the site described in Blumenberg et al. (2016). During a research cruise to the outer Hinlopen Strait in July 2018, hydro-acoustic flares from the seabed were detected with the ship echo-sounder from the same area as investigated by Geissler et al. (2016) in water-depths of ~330–350 m. A flare was recorded at the crest of a small ridge on the eastern flank of Hinlopen Trough (Rasmussen et al., 2018b) and gravity coring revealed sediment consisting of glaciomarine deposits on till. The coring site was revisited during a cruise with R/V *Helmer Hanssen* (UiT – The Arctic University of Norway, Tromsø) in September 2018 and hydro-acoustic flares were again detected with the ship echo-sounder. Onsite, box core-samples were retrieved from the area with flares and used for faunal and sediment analyses in this study (Rasmussen et al., 2018a) (Figure 2).

## Sampling

Samples from the five above mentioned methane seep locations were sampled with R/V *Helmer Hansen* and additional non-seepage stations P1 to P5 were sampled with R/V *Kronprins Haakon* (The Norwegian Polar Institute, Norway). Samples were collected during Arctic summer 2014–2018, i.e. late May–June for W. Svalbard seeps, late June–July for

SW. Barents Sea seeps and mid-late August to 2<sup>nd</sup> of September for N. Barents Sea seeps (Figure 1). Some temporal variation in seepage (Ferré et al., 2020) and uptake of chemosynthesis-based carbon between sampling events cannot be excluded, however, all sampling took place in the post-spring bloom period. Furthermore, long isotopic turnover (Kaufman et al., 2008; Weems et al., 2012) and high longevity of Arctic invertebrates (Bluhm et al., 1998; Ravelo et al., 2017) will dampen temporal variations. Our results were combined for all samples.

Seabed bathymetry mapping was conducted with ship-mounted multi-beam and 2D seismic surveys. Locations of active hydrocarbon seepage were selected based on acoustic signals from flares detected on a keel mounted single beam echo sounder (Simrad EK 60 frequencies 18 KHz and 38 KHz) and from previous surveys at the different sites (Åström et al., 2016; Serov et al., 2017). Benthic sampling in 2014 was conducted where acoustic reflections from flares were observed [see detailed description in Åström et al. (2016)]. During 2015, samples were collected where characteristic seep features such as bubble streams, microbial mats and methane-derived authigenic carbonates (hereafter referred to as carbonate outcrops) were identified through seafloor imagery. Images were obtained with a towed camera, mounted on a camera guided multi corer (cores diameter 10 cm) (see details in Åström et al. (2018)). In 2016, benthic

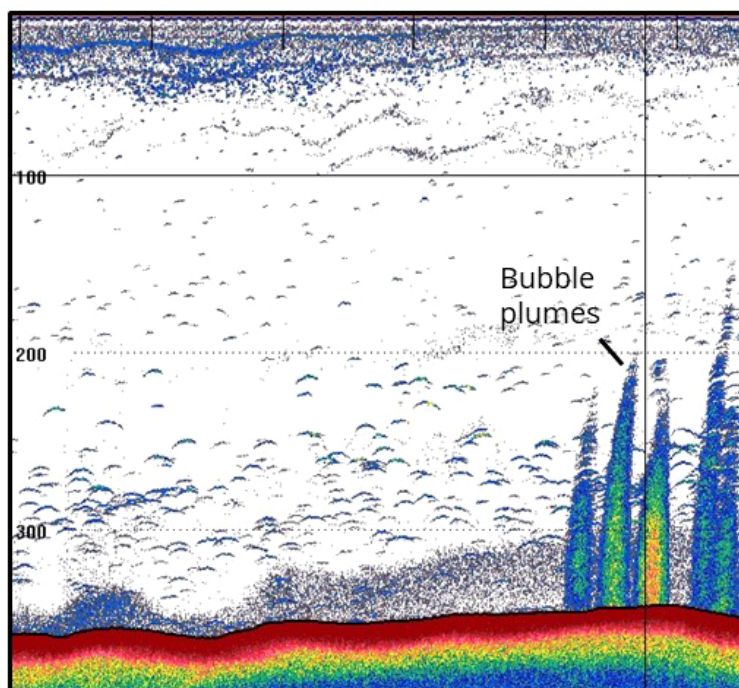


FIGURE 2

Echo-sonar image of seabed and acoustic flares from Hinlopen seep (HLF), north of Svalbard, recorded with a Simrad EK 60 single-beam echo sounder. Note that the bubble flares rise more than 150 m vertically from the seabed into the water-column. Elongated shapes indicate fish (and possible other larger organisms in the water column). Vertical scale to the left represents water depth (m).

sampling and seafloor imaging were carried out using the remotely operated vehicle 30K, operated by the Norwegian University for Science and Technology. Video recording and a pair of stereo cameras (image resolution 1360 x 1024 pixels) allowed to pinpoint areas of active gas bubbling, detailed studies of the seafloor structures including carbonate outcrops and microbial mats, and precise sampling at these features, see details in Åström et al. (2019). In 2018, a box corer (50x50x50 cm) was used to sample previously known seeps in the Barents Sea as well as the newly discovered seep site at outer Hinlopen Trough on the northern shelf of Svalbard. Along with sampling at active seep-sites, we also conducted sampling at paired non-seep controls in 2014–2018. In 2018, sampling with benthic trawls and box corer (50x50x50) was also carried out onboard R/V *Kronprins Haakon* along the South-North transect of the Norwegian project “Nansen Legacy” at latitude ~31–34°E from the central Barents Sea, moving northwards into the marginal ice-zone (Figure 1).

Vertical CTD (Conductivity, Temperature, Depth; SBE 9 plus sensor) profiles of seawater hydrography were taken at all stations prior to sampling and water was taken from attached Niskin bottles for analysis of pelagic particulate organic matter (POM). Moreover, sediment samples were obtained to analyze sediment characteristics such as porosity, grain size, total organic carbon, composition of isotopes ( $^{13}\text{C}$  and  $^{15}\text{N}$ ) and benthic pigments (Chlorophyll *a* and phaeopigments). At each location, qualitative faunal samples were collected from grabs, cores, manual remotely operated vehicle-Sampling or dredges for bulk stable isotope ( $\delta^{13}\text{C}$  and  $\delta^{15}\text{N}$ ) analyses of tissue to assess food web and trophic level interactions (Hobson and Welch, 1992; Post, 2002; Søreide et al., 2006). After sieving, to separate sediment from fauna, animals for isotopic analysis were sorted and identified to lowest possible taxonomic level immediately after collection, and we hereafter follow the names according to world register of marine Species (WoRMS Editorial Board, 2022). For some taxa (primarily for mud-dwelling echinoderms), we added a 1–2 day period of depuration in a dark cold-room onboard the vessel. Organisms were stored frozen (-20 °C) prior to laboratory analysis.

### Stable isotope analyses

For stable isotopic analyses, smaller organisms were processed whole whereas soft tissues from larger individuals were separated from other body structures, such as shells and guts. Tissues were freeze-dried for 24 hours, and dried tissue was homogenized with mortar and pestle and ~1.2 mg tissue sample<sup>-1</sup> weighed into tin capsules (containing between 0.3 and 0.7 mg carbon and 0.1 to 0.2 mg nitrogen). Calcareous organisms, where no soft tissue could be dissected, were pre-treated with 1N HCl and dried at 60°C ahead of carbon isotopic analysis to avoid contamination by eventual diagenetic carbon in the  $\delta^{13}\text{C}$  signature. For the same reason, sediment samples were acidified with HCl and dried before the carbon analysis. 5 mg sediment

sample<sup>-1</sup> was weighed into tin capsules for C-analyses and ~20 mg for N samples. POM isotopic signature measurements were derived from seawater filtered onto pre-combusted membrane filters (0.22 µm pore size, 4.7 cm diameter, Merck Millipore). In total, we use ~250 analyzed samples for this study. In addition, to expand the data set, we also include previous data collected from above-mentioned cold seeps reported in Åström et al. (2019).

For stable isotope analysis of bulk organic samples (sediment, tissue, and POM), we used a Thermo Fisher Scientific EA IsoLink IRMS System at the University of Oslo, Norway, which consists of a Thermo Fisher Scientific Flash Elemental Analyzer and a Thermo Fisher Scientific DeltaV Isotope Ratio Mass Spectrometer. Quality control for the analyses with external standards was better than ±0.16‰ for  $\delta^{15}\text{N}$  and better than 0.5‰ for  $\delta^{13}\text{C}$ . Isotopic compositions are reported in the conventional  $\delta$ -notation, as  $\delta^{15}\text{N}$  and  $\delta^{13}\text{C}$  in ‰ relative to air and Vienna Pee Dee Belemnite, respectively.

### Sediment analysis

Sediment samples were collected for benthic chlorophyll *a* (Chl *a*) and phaeopigments, as indicators of photosynthetically based organic material deposited on the seafloor. Sediment chlorophyll *a* indicates relatively recently produced material, whereas phaeopigments represent a degradation product of chlorophyll *a*. Surface sediment pigment concentrations (upper 0–2 cm) from grab samples and push cores were extracted with acetone for 12–24 h in the dark, centrifuged, decanted and measured for fluorescence in a Turner Design Model 10 AU fluorometer before and after acidification with 1N hydrogen chloride (HCl) in accordance with Holm-Hansen et al. (1965) The measured concentrations were corrected for sediment porosity. We use the term chloroplastic pigment equivalents for the combined concentration of Chl *a* and phaeopigments in this study (Pfannkuche and Thiel, 1987).

Porosity of sediment samples was determined by using a wet-dry method where pre-weighed vials of known volume were filled with sediment, re-weighed, and later dried at 60° C until all water evaporated. The density of the sediment was calculated by using the basis from the wet weight of sediment and water combined following Zaborska et al. (2008). Sediment grain size (fraction of pelite <0.63 µm) and total organic carbon were determined by subsampling surface sediments (0–2 cm). Grain size was analyzed in a Beckman Coulter Particle Size analyzer LS 13320. Samples were pre-treated with 1N HCl and H<sub>2</sub>O<sub>2</sub> to remove CaCO<sub>3</sub> and organic material. Total organic carbon was analyzed by first determining the total carbon content in a Leco CS744 instrument that uses infrared absorption to measure generated CO<sub>2</sub> under combustion. Samples were then treated with HCl to remove inorganic carbon. The analyzed difference between treatments is used to calculate the content of Total Organic Carbon in the sediment.

## Data analysis

Photosynthetic particulate organic matter was used as the isotopic baseline (nitrogen) for estimating trophic level. To illustrate overall trophic structure the trophic level fractionation value was set to 3.4‰ for N and 0.6‰ for C following Zanden and Rasmussen (2001); Post (2002) and Søreide et al. (2006) according to the formula:

$$\text{Trophic Level} = ((\delta^{15}\text{N}_{\text{cons.}} - \delta^{15}\text{N}_{\text{POM}})/3.4) + 1$$

Where  $\delta^{15}\text{N}_{\text{cons.}}$  represents the nitrogen value for a given taxon and  $\delta^{15}\text{N}_{\text{POM}}$  represents the mean particulate organic matter (POM) baseline nitrogen value in this study ( $\delta^{15}\text{N}=5.1\text{‰}$ ).

To test the hypothesis that chemosynthesis-based carbon contributes to various fauna at seep sites, we used benthic organisms that exhibited lower  $\delta^{13}\text{C}$  values than the baseline of POM ( $\delta^{13}\text{C} = -24.5\text{‰}$ , Table S1) in a two-component mixing equation. This analysis provided an estimate of the contributed fraction of the two carbon sources, photosynthetic particulate organic matter, POM and chemosynthesis-based carbon, based on the  $\delta^{13}\text{C}$  values from sampled organisms using the formula:

$$X_{\text{fraction}} = (C_{\text{cons.}} - C_{\text{POM}})/(C_{\text{chemo}} - C_{\text{POM}})$$

$C_{\text{cons.}}$  is the  $\delta^{13}\text{C}$  value of a specific organism,  $C_{\text{POM}}$  represents the mean baseline value of photosynthetic carbon sources and  $C_{\text{chemo}}$  is the baseline value from chemosynthetic carbon sources. To estimate the contribution of chemosynthesis-based carbon, we tested the two-component mixing equation with two different  $C_{\text{chemo}}$  key end-members, 1) methane ( $\text{CH}_4$ ) and 2) sulfur oxidizing bacteria (SOB).  $C_{\text{chemo}}$  for methanotrophs is based on a mean of published values of isotopic analyses of methane gas composition from the Svalbard-Barents Sea region ( $\delta^{13}\text{C}=-44.0\text{‰}$ , see Table S1) whereas  $C_{\text{chemo}}$  for thiotrophs ( $C_{\text{SOB}}=-35.0\text{‰}$ ) is based on an average of published SOB values in Decker and Olu (2012) and Gebruk et al. (2003) and integrated reduced sediment and bacterial mat samples from Åström et al. (2019). We also apply the two-component mixing equation (2) using sedimentary organic matter (SOM) as baseline (mean value of  $\delta^{13}\text{C} = -21.8\text{‰}$ ) to account for the modification of pelagic POM during transit to the seafloor. Sedimentary organic matter includes refractory particulate organic matter at different levels of degradation and diagenesis (Schubert and Calvert, 2001), allowing a more refined estimate of the extent to which different organisms have incorporated carbon from chemosynthetic sources (e.g. Zapata-Hernández et al., 2014). A pairwise comparison of  $\delta^{13}\text{C}$  values of the two photosynthetic carbon sources (POM and SOM) satisfied the conditions of normality and equal variance and differences were tested using a Student's t-test.

To further test the hypothesis that chemosynthesis-based carbon contributes to the overall background benthic community we used 'SIBER' (Stable Isotope Bayesian Ellipses in R version 4.0.5) (Jackson et al., 2011) and selected Layman metrics (Layman et al., 2007) to quantify isotopic niche characteristics of habitats for 'seeps areas' and 'non-seeps' in the Barents Sea. Isotopic niche space was compared between two habitat groups and five taxonomic groups; 'Polychaeta', 'Echinodermata', 'Mollusca', 'other benthos' (including among others demersal crustaceans and fishes, priapulids, nemerteans and cnidarians) and 'pelagic community' (including pelagic taxa e.g. krill and pelagic amphipods), see details for categorical classification in supplementary material (Table S2). We excluded chemosymbiotic siboglinids from the 'Polychaeta' group as they derive their nutrition *via* microbial endosymbionts (Sen et al., 2018b) and the purpose in this analysis was hence to compare non-chemosymbiotic fauna from the two community-groups. We calculated the nitrogen range (NR) in order to look at the length of the food web (accordingly  $\text{NR } \delta^{15}\text{N}_{\text{max}} - \delta^{15}\text{N}_{\text{min}}$ ), and carbon range (CR) to assess basal niche diversification, where large a large CR indicates multiple basal resources (accordingly  $\text{CR } \delta^{13}\text{C}_{\text{max}} - \delta^{13}\text{C}_{\text{min}}$ ). We computed isotopic niche space as total area of the convex hull and standard ellipse area for the bivariate  $\delta^{13}\text{C}:\delta^{15}\text{N}$  data. Furthermore, we determined the standard ellipse area overlap between the means for isotopic niche area for seep and non-seep sites and between the taxonomical categories from the respective community. Total area is used as a proxy for the total isotopic niche of all consumers of a specific community while the convex hull is highly influenced by extreme values. We retain however the total area here as it provides an overview of the total isotopic niche space and includes all sampled organisms in the study. Standard ellipse area, in contrast, is a proxy for a core isotopic area, and is hence smaller than Total Area and less sensitive to outliers and extreme data points (Layman et al., 2007; Jackson et al., 2011). A large total area or standard ellipse area value indicate a larger isotopic niche.

The environmental data were analyzed and used to further test the hypothesis that the shallow, productive, seeps are less influenced by chemosynthesis-based carbon in comparison to the deeper seeps at the shelves. We performed a pairwise comparison (t-test) of sediment Chl *a* to the total chloroplastic pigment equivalents ratios between seep and control station to test for differences in food quality (i.e. fresh and recently produced to older and partially degraded). To demonstrate the conditions of environmental variables at the different stations we used R and the package "vegan" v.2.5-7 (Oksanen et al., 2019) to run a principal component analyses. The selected environmental variables were bottom-water temperature, salinity, and sediment characteristics (including grain size, total organic carbon content, porosity of sediments) and total concentration of

benthic chlorophyll pigments. Data were normalized prior to analysis.

## Results

### Trophic structure at seep versus non-seep sites

Carbon isotope ( $\delta^{13}\text{C}$ ) values exhibited a wide range (-51.3 to -15.0‰,  $n = 381$ ) among studied taxa (Table S2). The most individual  $^{13}\text{C}$ -depleted samples were recorded in the chemosymbiotic siboglinid worms ranging between -51.3 and -32.7‰ ( $n$  samples = 12). Among non-chemosymbiotic taxa, the most  $^{13}\text{C}$ -depleted individual samples were recorded in large polychaetes collected at the seeps, *Scoletoma fragilis*,  $\delta^{13}\text{C} = -35.0\text{‰}$  and *Nephtys* sp.  $\delta^{13}\text{C} = -31.4\text{‰}$ . The highest  $\delta^{13}\text{C}$  values were recorded from two echinoderms: the sea star *Pontaster* sp. (-15.0‰) and the brittle star *Ophiopholis aculeata* (-15.5‰; Table S2). The majority of faunal samples in this study displayed  $\delta^{13}\text{C}$  values in the range of -22‰ to -16‰ (Table S2). The baseline carbon source of photosynthetic particulate organic matter (POM) from the water-column ranged between  $\delta^{13}\text{C} = -27.3\text{‰}$  and -23.3‰ and in sediment organic matter (SOM), for samples without signs of active seepage at the seabed,  $\delta^{13}\text{C}$  varied between -23.8‰ and -20.5‰. There was a significant difference between POM and SOM values, ( $t(18) = 4.3, p < 0.001; \text{mean}_{\text{SOM}} = -21.8 \pm 0.35 \text{ SE vs. mean}_{\text{POM}} = -24.5 \pm 0.56 \text{ SE}$ ). Two sediment samples collected at microbial mats and  $\text{H}_2\text{S}$  patches at seeps were depleted in  $^{13}\text{C}$  in comparison to other sediment samples,  $\delta^{13}\text{C} = -25.3\text{‰}$  and -34.5‰ respectively (Table S1).

Nitrogen isotope ( $\delta^{15}\text{N}$ ) values for the photosynthetic baselines where  $\text{mean}_{\text{POM}} = 5.1\text{‰} \pm 0.38 \text{ SE}$  and  $\text{mean}_{\text{SOM}} = 4.8\text{‰} \pm 0.13 \text{ SE}$  (Table S1). First order consumers (Trophic Level = 2) included pelagic invertebrates such as euphausiids (krill) and hyperbenthic amphipods (*Onisimus* sp.) as well as filter-feeding bivalves e.g. *Serripes groenlandicus*, *Macoma calcarea*, and *Ciliatocardium ciliatum* (Table S2). In addition, a few individuals of different echinoderms including the sea cucumber *Molpadia borealis* and

the sea urchin *Strongylocentrotus* sp. also exhibited low  $\delta^{15}\text{N}$  values, indicative of grazers (Table S2). The nitrogen isotope analysis revealed that most taxa were 2<sup>nd</sup> or 3<sup>rd</sup> order benthic consumers at Trophic Level ~3–4, containing typical deposit feeders, opportunists, and predators. We noted that the benthic fish species Atlantic poacher (*Leptagonus decagonus*) and American plaice (*Hippoglossoides platessoides*) were represented as top consumers in this study with individual samples of  $\delta^{15}\text{N} = 15.1\text{‰}$  and Trophic Level = 4 (Table S2). Food-web length as indicated by the range of nitrogen isotopic values was hardly any different between seep- and non-seep stations; nitrogen isotopic range = 9.88‰ and 9.62‰ respectively. In contrast, the carbon isotope range was almost double at seep stations compared to non-seep stations; carbon isotope range = 19.93‰ and 9.85‰ respectively. Comparing taxonomic/functional categories from non-seeps/controls to seep-stations, the total area and standard ellipse area were larger at seeps for three out of the five categories, where the exceptions are ‘Mollusca’ and ‘other benthos’ (Table 2). In all taxa combined, the calculated standard ellipse area-niche overlap between the seep-community and non-seep community was 65.2% (Figure 3). The least overlap was seen between ‘Polychaeta’, 38.0% and the most for ‘Mollusca’, 51.6%.

### Intra-species variation in isotopic composition

A few benthic taxa display large intra-species variability in their carbon values (Figure 4). The largest spread in species-specific carbon isotope composition was demonstrated within the polychaeta species of *Scoletoma fragilis* where individuals collected at the Gas Hydrate Mound seep station in Storfjordrenna differed by 16‰ from  $\delta^{13}\text{C} = -35.0\text{‰}$  to -18.9‰, ( $n = 4$ ), revealing a large variability within the same site. The variability among all collected *S. fragilis* in the study ranged from  $\delta^{13}\text{C} = -35.0\text{‰}$  to -18.6‰, ( $n = 10$ ). Furthermore, in *Nephtys* sp. there was also a large intra-site variation in  $\delta^{13}\text{C}$  at the Bjørnøyrenna seeps, varying by more than 14‰ (-31.4‰ to -17.1‰,  $n = 9$ ). For all sampled and analyzed *Nephtys* sp. regardless station, the range of  $\delta^{13}\text{C}$  was -31.4‰ to

TABLE 2 Total area, TA (‰<sup>2</sup>) and calculated standard ellipse area, SEA (‰<sup>2</sup>) for respective categorical group from the two communities “non-seep” and “seep”.

Taxonomical category	Polychaeta		Echinodermata		Mollusca		Other benthos		Pelagic	
	Non-seep	seep	Non-seep	seep	Non-seep	seep	Non-seep	seep	Non-seep	seep
Community										
Total area (TA) ‰ <sup>2</sup>	14.8	60.2	21.8	61.5	43.4	30.4	35.5	30.2	18.2	28.1
Standard ellipse area (SEA) ‰ <sup>2</sup>	7.9	16.0	8.1	14.8	11.3	7.5	11.3	7.2	9.1	11.6
SEA niche overlap between non-seep and seep categorical groups (%)	38		49		52		45		42	

Calculated SEA proportion shows the niche overlap between categorical groups from respective community, presented here as percentage of overlap.

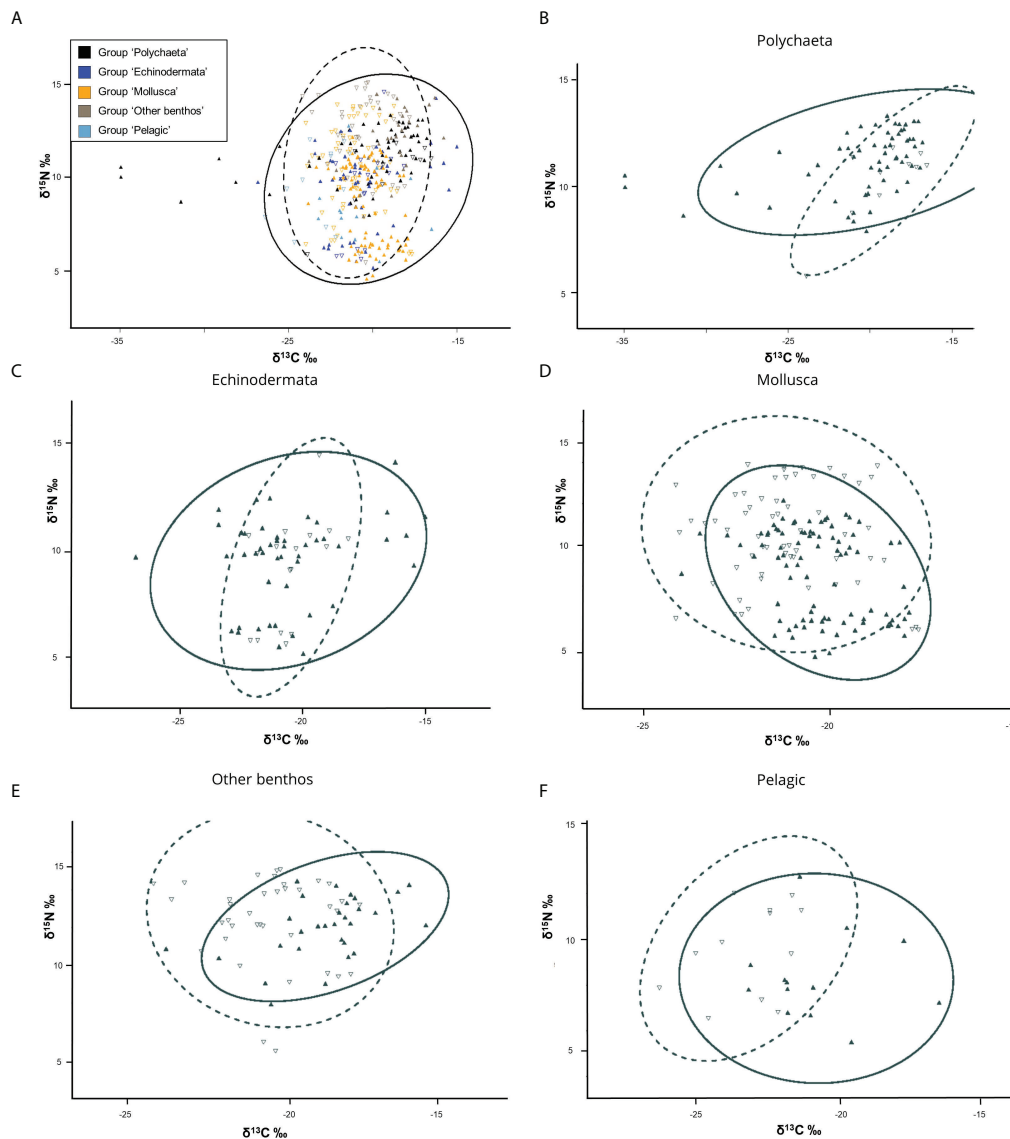


**FIGURE 3**  
 Isotopic data of consumers plotted in bivariate C:N δ-space. Ellipses show standard ellipse area (SEA) of bivariate means for non-seep (dashed line) and seeps (solid). Open triangles represent samples collected from non-seeps, solid symbols indicate samples collected at seeps. **(A)** All samples. Calculated niche overlap of SEA is 65% between seeps vs. non-seeps. **(B–F)** SEA of bivariate means for taxonomic/functional groups. Calculated overlap in SEA between groups **(B–F)** is found in [Table 2](#). Note the different x and y-scales.

-16.5‰ ( $n = 31$ ) Among non-Polychaeta taxa, the mud-dwelling sea star *Ctenodiscus crispatus* displayed the largest intra-species variability in individual samples where the  $\delta^{13}\text{C}$  ranged between -26.8‰ and -16.6‰, ( $n = 21$ ) (Figure 4). In contrast to the carbon values, the nitrogen values varied little and there was no consistent difference between seeps and non-seeps. The exception for an extraordinarily high variation in  $\delta^{15}\text{N}$  was seen in the sea cucumber *Molpadia borealis*, where  $\delta^{15}\text{N}$  values ranged from 5.8‰ to 14.6‰, ( $n = 9$ ). Both the low and high extremes were collected at non-seep sites.

### Chemosynthesis-based carbon end-member contributions

The results from the two-component mixing equation using  $C_{\text{POM}}$  and  $C_{\text{chemo}}$  as end-members indicate that a suite of non-chemosymbiotic taxa, the majority of them polychaetes, incorporated carbon from chemosynthesis-based carbon (up to 54%–100%) (Table S3; Figure 5).

Using sedimentary organic carbon as a primary carbon source, instead of  $C_{\text{POM}}$  to the end-member

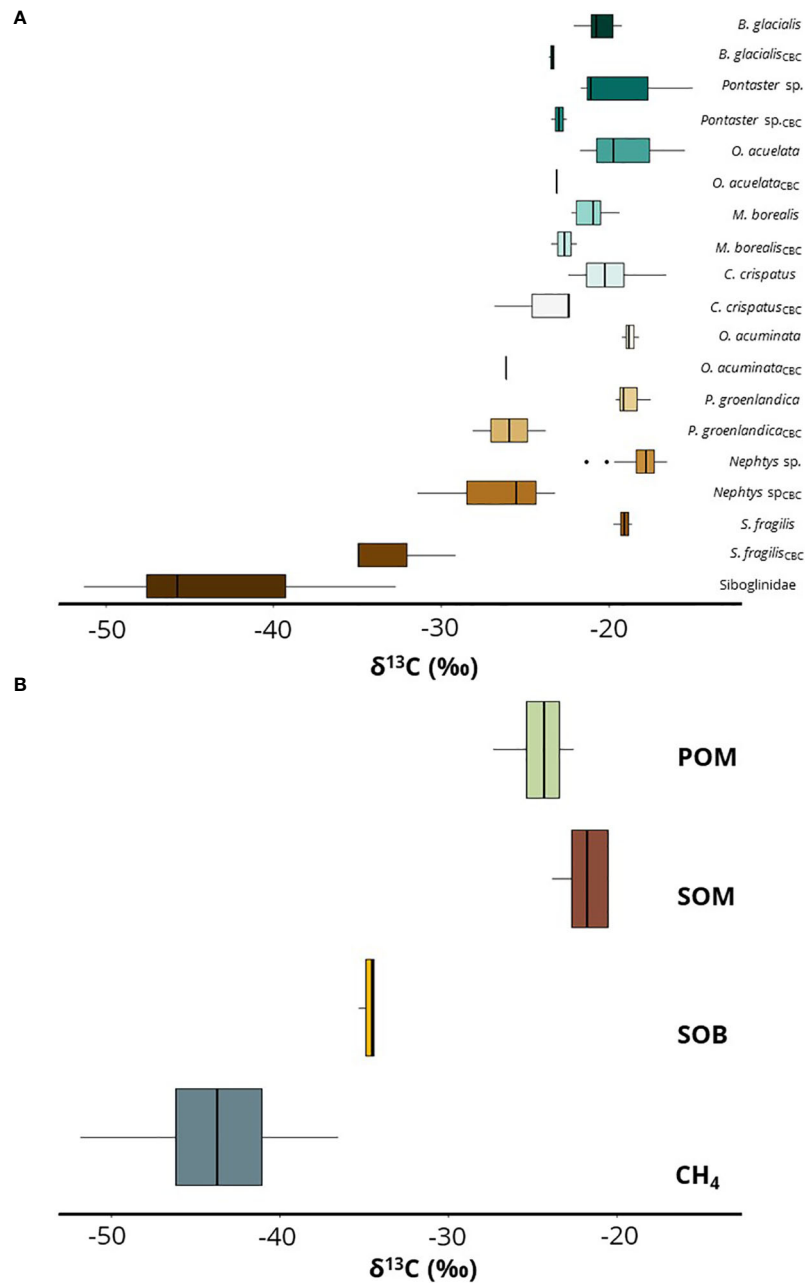
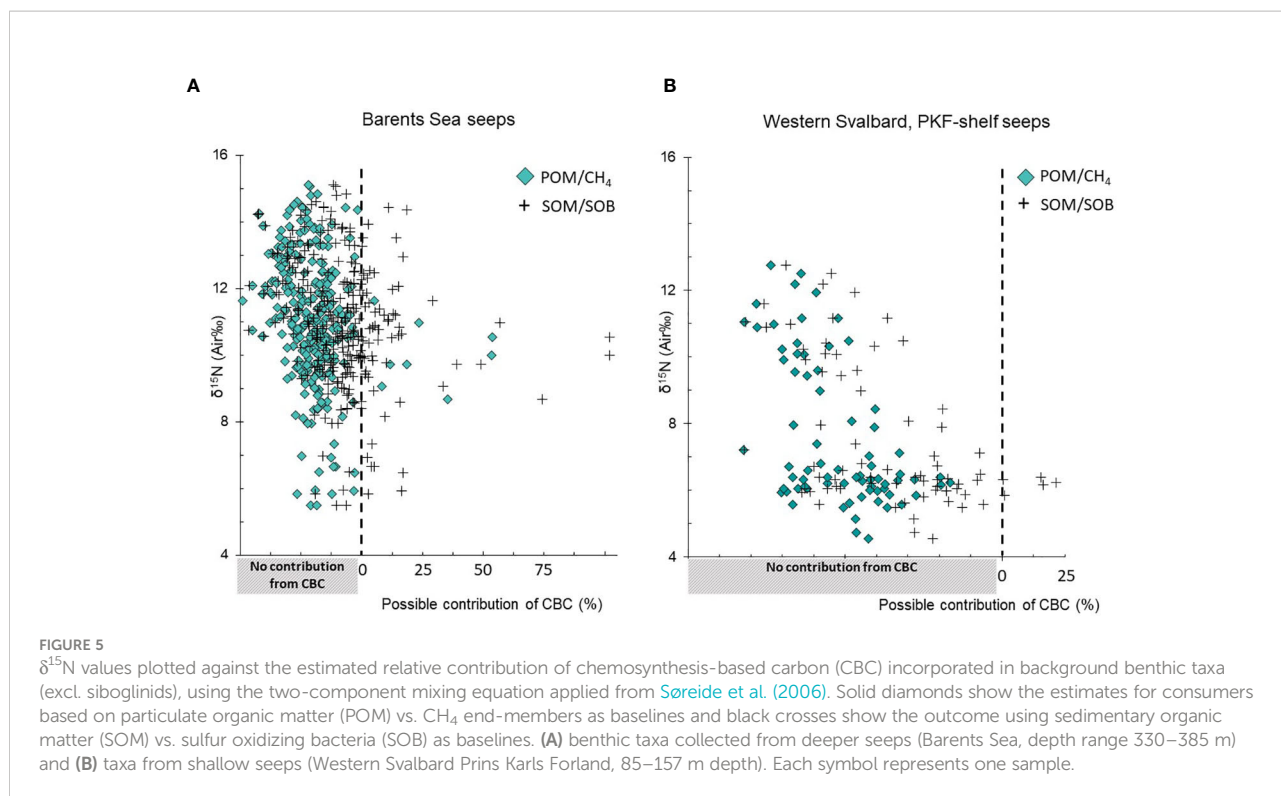


FIGURE 4

Boxplots of  $\delta^{13}\text{C}$  variation in selected benthic invertebrates and community baseline sources. (A) Intra-specific comparisons of benthic taxa and measured  $\delta^{13}\text{C}$  values in this study. (B)  $\delta^{13}\text{C}$  ranges of baseline energy-sources at the investigated area, abbreviations; CH<sub>4</sub>-methane, SOB-Sulfur oxidation bacteria, SOM-sediment organic matter, POM-particulate organic matter (water-column). The bold line represents the median value, the edges of the box represent the 25<sup>th</sup> and 75<sup>th</sup> percentile of data and the solid line display the highest and lowest values excluding outliers (black dots outside box). Reference data from Svalbard for *O. acuminata* is based on Renaud et al. (2011) and for *P. groenlandica* on (Sokołowski et al., 2014; Renaud et al., 2015). *B. glacialis*, *Bathycarca glacialis*; *O. aculeata*, *Ophiopholis aculeata*; *M. borealis*, *Molpadia borealis*; *C. crispatus*, *Ctenodiscus crispatus*; *O. acuminata*, *Ophelina acuminata*; *P.groenlandica*, *Phyllodoce groenlandica*; *S. fragilis*, *Scoletoma fragilis*.

equation (i.e. C<sub>SOM</sub>) to CH<sub>4</sub> resulted in a similar range of contributions of chemosynthesis-based carbon for benthic invertebrates (up to 59%–100%). Applying the latter scenario of the mixing model using SOM and SOB as

end-members showed in the mixing model that a partial input of the diet for several benthic organisms could be composed of chemosynthesis-based carbon-derived sources, also beyond polychaetes; Echinodermata (up to



39%), Mollusca (up to 16%), Priapulida (15%) and Pycnogonida (<5%) (Table S3).

Estimates of chemosynthesis-based carbon in individuals varied between depth groups. Individuals collected at deeper (Barents Sea) seeps displayed a larger modeled input of chemosynthesis-based carbon (up to 50–100%) in comparison to taxa and individuals collected at the shallower seeps (Prins Karls Forland shelf-seeps in Western Svalbard). In fact, hardly any depleted  $^{13}\text{C}$  values and thus, no chemosynthesis-based carbon contributions, were detectable in organisms at the latter site (Figure 5B).

### Environmental conditions

In the principal component analysis over environmental variables, stations were overall ordinated regionally, demonstrating the influence on stations of selected environmental variables (Figure 6). Western Svalbard shelf stations were separated from Barents Sea stations along the first principal component analysis-axis, explaining 51.3% of the variability in the data where the characteristics of water-mass (temperature and salinity) and sediments (grain size, total organic carbon and porosity) caused the observed difference. The two northernmost stations, Hinlopen seep site (HLF, north of Hinlopen strait) and P4 (south of Kvitøya; Figure 1) were

ordinated at opposite edges along the second principal component analysis-axis (explaining 21.7% of the variability in the data) and the observed separation was explained by differences in water temperature and content of chloroplastic pigment equivalents (Figure 6). P4 displayed the coldest water-mass at the bottom, ( $T = -0.2^\circ\text{C}$ ) and  $S = 34.8$  psu, characteristic of Arctic water (Svendsen et al., 2002) (Table 1), and was the only station with negative bottom-water temperature. In contrast, Hinlopen Flare site was the second warmest station ( $T = 3.5^\circ\text{C}$ ) and influenced by warm and saline (35 psu), Atlantic water. For chloroplastic pigment equivalents in the sediment, the concentration was highly variable among stations and there was no significant difference in total pigment concentration between seep and non-seep stations. The stations Hinlopen Flare site and P1, ordinated in the upper range of the y-axis (Figure 6) displayed the highest concentrations of chloroplastic pigment equivalents in the sediment. We detected a significant difference in the ratio of sediment chlorophyll *a* (Chl *a*) to sediment chloroplastic pigment equivalents concentration, where seeps had a lower ratio of Chl *a* compared to non-seep control stations;  $t(56) = 2.129$   $p < 0.05$   $\text{mean}_{\text{control}} = 0.222 \pm 0.008$  SE vs.  $\text{mean}_{\text{seep}} = 0.197 \pm 0.007$  SE. For total organic carbon content, we noted a trend towards slightly higher Total Organic Carbon concentration in sediments at seep-stations, however, the difference was too small to exclude the natural variability ( $t$ -test,  $p > 0.05$ ).

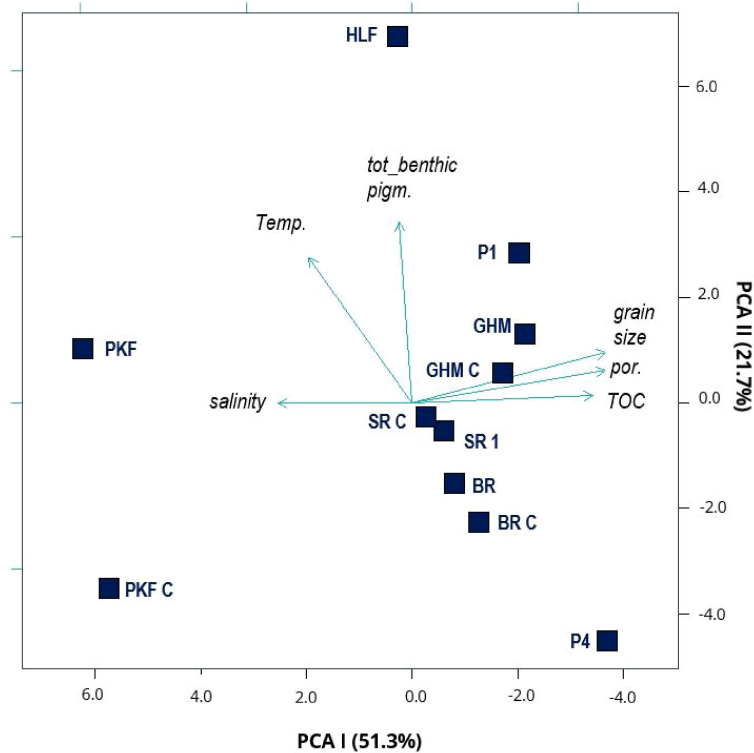


**FIGURE 6**  
 Principal component analysis based on standardized environmental variables; Bottom water temperature (Temp), salinity and sediment characteristics (including grain size, total organic carbon (TOC), porosity (por.) of sediments) and total concentration of benthic chlorophyll pigments from sampled station in this study. (No sediment and pigment data were obtained from P2, P3 and P5, see details in Table 1 for station information). There is a clear regional separation between Western Svalbard Prins Karls Forland stations (PKF and PKF C), compared to stations in the Barents Sea region (all others) as these stations are diverged along the first principal component analysis axis (PCA I), primarily related to the variable’s salinity and sediment characteristics, explaining more than 50% of the observed difference. North of Svalbard, the station Hinlopen seep site (HLF) and station P4 at the northern Barents Sea shelf are separated along PCAII, mainly driven by the contrasting bottom water temperatures and sediment pigment concentration. For site abbreviations see Table 1.

## Discussion

Cold seeps and chemosynthesis as potential energy sources for Arctic benthos have in the past been rather uncertain or entirely overlooked. This is in contrast to other identified carbon sources which are included in the Arctic benthic food-web such as terrestrial sources as well as phytoplankton, macro-, and ice algae production (e.g. Søreide et al., 2006; Sokołowski et al., 2014; Renaud et al., 2015). We demonstrate, in this study, that a variety of “background” benthic taxa at the investigated cold seeps can benefit from carbon sources originating from chemosynthesis-based carbon (CBC). We detect a larger isotopic niche-width for seep-communities than non-seep communities and report intra-species variability in isotopic carbon signals, reflecting the availability of multiple carbon sources to the community and flexible feeding-patterns among benthic taxa. Furthermore, we note contrasting patterns in the use and incorporation of chemosynthesis-based carbon between

shallow seeps at the Western Svalbard margin and deeper ones at the Barents Sea shelf. Despite intense methane seepage from the bottom at the shallow sites, we did not recognize much use of chemosynthesis-based carbon in ambient background taxa. We suggest this may be a result of an intensified photosynthetic production, caused by local seep-mediated upwelling and high pelagic-benthic coupling at the shallow seep sites.

## Community comparisons of trophic structure at seep and non-seep sites

We confirm our hypothesis that chemosynthesis-based energy sources are incorporated in a suite of benthic organisms. We detected highly depleted <sup>13</sup>C values in primarily benthic predatory polychaetes. With recorded values of -35.0‰ in δ<sup>13</sup>C and trophic levels of 2–3 for invertebrates

collected at the seeps, it is unlikely that these individuals would have incorporated these low values through other sources. We expected negligible input from terrestrial sources (from land-riverine discharge) and no significant input of macroalgae, that could cause such low  $\delta^{13}\text{C}$  values (Renaud et al., 2015; Bell et al., 2016; McGovern et al., 2020) considering the depth and distant location to land of our sampling locations. The overall isotopic niche space in a specific habitat represents the heterogeneity of carbon use. While the length of the food-webs did not differ between seeps and non-seep samples in this study, the main difference between the communities is seen in the range of  $\delta^{13}\text{C}$  values. A higher  $\delta^{13}\text{C}$  range indicates availability of diverse basal resources and/or a potential diversity in the isotope values of these basal sources (Layman et al., 2007). The observed larger carbon isotope range for the seep community in this study is hence reasonable considering the additional available carbon sources *via* chemosynthesis and hydrocarbon seepage. Among taxonomic/functional groups, we saw a considerably larger isotopic niche space (expressed as total area and standard ellipse area) for 'Polychaeta' and 'Echinodermata' at seeps in contrast to non-seeps, consistent with these groups having individuals with the largest estimated proportions of chemosynthesis-based carbon (Table S3). The relative high proportion of isotopic niche overlap between the two communities (seeps and non-seeps) as a whole, and among the categorical taxonomic groups, suggests that they share a high proportion of basal food resources (McTigue and Dunton, 2017). This is also a realistic as well as an expected result as the seep and non-seep communities were composed of the same species overall and given the fact that the investigated seeps lack higher trophic level chemosymbiotic faunas beyond siboglinids (which were excluded in the niche space analysis). Moreover, we found in general a relatively high utilization of particulate organic matter and sediment organic matter carbon sources among the analyzed organisms. The least overlap between the two communities was observed in 'Polychaeta', highlighting the large variance in  $\delta^{13}\text{C}$  signals within this group, indicative of multiple available carbon sources (Figure 3).

The large intra-species variability in carbon signals in a few taxa likely reflects the flexibility in utilization of food resources within the investigated species. For example, the species-specific difference of  $\sim -15\text{‰}$  in  $\delta^{13}\text{C}$  in each of the two species of polychaetes, *Scoletoma fragilis*, and *Nephtys* sp., suggests that these species feed from a variety of carbon pools at the sea floor. Furthermore, it indicates that the  $^{13}\text{C}$ -depleted individuals consume prey or organic matter with a chemosynthetic origin. Our finding is consistent with the general observation at cold seeps and other reduced habitats that utilization and incorporation of chemosynthetic carbon occurs also in non-chemosymbiotic taxa showing that non-specialists can benefit from such additional carbon sources (Levin and Michener, 2002; Bernardino et al., 2012; Zapata-Hernández et al., 2014). A few studies have now documented this phenomenon in Arctic waters

(Gebruk et al., 2003; Decker and Olu, 2012; Sweetman et al., 2013) where the most common macro-benthic taxonomic groups that incorporate chemosynthesis-based carbon are polychaetes, mollusks and echinoderms. In this study, we establish that a larger number of taxa than previously known appears to incorporate carbon sources derived *via* chemosynthesis at Arctic seeps, including large predatory polychaetes such as lumbrinerids, nephtyids and phyllodocids, which can derive significant proportions of chemosynthesis-based carbon at seeps.

## Photosynthetic production at seeps

Characteristic for Arctic shelves with inflow of Atlantic Water is high primary production and strong pelagic-benthic coupling, hence the fraction of surface production reaching the benthic community is high for the investigated areas (Grebmeier and Barry, 1991; Wassmann et al., 2020). We noted in this study that the larger portion of the benthic community utilized photosynthetically produced carbon sources despite a high potential for cold seeps to fuel marine systems. Previously, it has been argued that the amount of surface photosynthetic primary production and fraction of vertical particulate flux to the seabed can restrict the development of chemosynthesis-dependent communities, including the settlement of chemosymbiotic species (Sahling et al., 2003; Vedenin et al., 2020). Hence, the results in this study are neither unexpected nor surprising given that utilizing chemosynthetic sources directly may imply costly physiological adaptations. In order to avoid sulfide intoxication some animals have evolved special binding proteins to tolerate high sulfide concentrations in reduced habitats (Vismann, 1991; Terwilliger, 1998). Yet, if there is sufficient supply from photosynthetic resources, there is no essential need to develop such adaptations. Specifically, for the shallow Western Svalbard Prins Karls Forland seeps, no taxa stand out in carbon depletion that would be indicative of chemosynthesis-based carbon. Moreover, there are at present no records of siboglinid polychaetes from these seeps at depths shallower than 250 m (Sahling et al., 2014; Åström et al., 2016) despite intense and long-term methane seepage this area (Sahling et al., 2014; Portnov et al., 2016). We speculate that the reason why we do not find siboglinids (and other chemosymbiotic taxa) or detect any significant use of carbon sources derived *via* chemosynthesis in macrobenthos at these shallow Western Svalbard Prins Karls Forland seeps is the high primary production and the strong pelagic-benthic coupling: At the Western Svalbard Prins Karls Forland seeps, Åström et al. (2016) recorded the highest concentration of chloroplastic pigment equivalents in the sediment as well as the highest macrofaunal biomass (321 g wet weight  $\text{m}^{-2}$ ) in a comparative study of macrobenthic seep-communities between Western Svalbard and the Barents Sea. In our present study, we also infer strong pelagic-benthic coupling from the relatively high concentration of chloroplastic pigment equivalents at a few

stations. The significant *lower* ratio of sediment chlorophyll *a* to the total concentration of chloroplast pigments in the sediments at the seeps, in contrast to non-seep stations seen in this study, may imply that the available and the recently produced fresh organic material is more swiftly consumed by organisms at the seeps, reflected also in the high abundance and biomass there (Åström et al., 2016). Such links are consistent with earlier findings relating high vertical export of photosynthetic and biogenic material produced in surface-waters with high macrobenthic biomass (Ambrose and Renaud, 1995; Wei et al., 2011). Moreover, investigations by Pohlman et al. (2017) of the water-column and exchange of methane and carbon dioxide (CO<sub>2</sub>) across the sea–air interface at seeps at the Western Svalbard margin revealed that CO<sub>2</sub>-uptake in surface-waters was enhanced where elevated methane concentrations were recorded, in contrast to the surrounding waters. These authors suggested that physical mechanisms (e.g., upwelling) bring methane and possibly nutrient-enriched waters to the surface at seeps, which supports enhanced primary production and CO<sub>2</sub> drawdown in the surface-water (Pohlman et al., 2017). Furthermore, in the same area Sert et al. (2020) reported significant correlations between more bio-labile dissolved organic carbon and greater chemical diversity of dissolved organic carbon at seeps in comparison to non-seeps. Based on these findings, Sert et al. (2020) suggested that microbial processes at the seeps significantly influenced the composition of dissolved organic matter in the water column. The abovementioned examples support the arguments that in areas of high primary production, the photosynthetic effect overrides a potential chemosynthetic signal despite intense methane seepage.

On the contrary, in shallow water but in less primary-productive and oligotrophic systems, seepage seems to stimulate uptake of chemosynthetic carbon by macrobenthic communities at the seabed. This is observed from the Laptev Sea where shallow methane seeps (~ 60–70 m deep) support dense populations of chemosymbiotic species (*Oligobrachia* sp.) (Vedenin et al., 2020) and growth of microbial mats at the sea bed. In comparison to the productive inflow shelves at Western Svalbard (Wassmann et al., 2006), the Laptev Sea, as an interior shelf, is characterized by a narrow window of summer phytoplankton primary-production, while during the rest of the year it is ice-covered and the photosynthetic production remains extremely low (Sorokin and Sorokin, 1996; Vedenin et al., 2020). Also, at the Western Svalbard Prins Karls Forland seeps, microbial mats are observed at the bottom at 80 m water depth, yet, no larger chemosymbiotic macrofauna has been recorded (Sahling et al., 2014; Åström et al., 2016). The only background macrobenthic taxon that potentially may benefit directly from carbon sources derived *via* chemosynthesis in this area was the sea urchin (*Strongylocentrotus* sp.). Individuals of *Strongylocentrotus* sp. were observed sitting (potentially grazing) at microbial mats at the Western Svalbard Prins Karls Forland-seeps (Figure 7) although isotopic signatures did not indicate uptake of chemosynthesis-based carbon in collected specimens.

## Footprint of carbon sources derived *via* chemosynthesis and assimilation to benthos

In this study, we have shown that chemosynthesis-based carbon reaches macro-benthic communities beyond microbial assemblages and chemosymbiotic siboglinid worms. The use of carbon sources derived *via* chemosynthesis occurs not only at isolated deep-sea seeps with limited input of photosynthetic organic matter (e.g. Seabrook et al., 2019; Toone and Washburn, 2020; Ashford et al., 2021), but also takes place at highly productive Arctic shelves. We acknowledge, though, that the use of bulk stable isotopes is more insightful when combined with compound-specific isotope analysis (Niemann et al., 2013; Seabrook et al., 2019). For example, Seabrook et al. (2019) studied tanner crabs (*Chionoecetes tanneri*) inhabiting seeps along the North American west coast and used both bulk stable isotopes and compound specific isotope analyses to investigate the diet of crabs and found differing results. Their result from bulk stable isotopes analysis seemingly suggested that the crabs primarily relied on photosynthetically derived food resources since  $\delta^{13}\text{C}$  values in their tissue ranged between -20.5 and -17.4‰ (Seabrook et al., 2019). In contrast, the compound specific isotope analysis of bacterial fatty acids indicated chemosynthetic processes and methane-derived carbon. Furthermore, Seabrook et al. (2019) also noted high abundance of seep-associated microbes in guts of some tanner crabs indicating a direct consumption of seep associated bacteria and archaea. It is also likely that the level of mobility of higher trophic level taxa may influence the detection of potential chemosynthesis-based carbon in animal tissue. Highly mobile taxa could explore a larger variety of carbon sources available at seeps disguising a potential chemosynthetic carbon isotope composition. For example, in a study from seeps in the Gulf of Mexico, MacAvoy et al. (2003) noted that for a less mobile sea star, the carbon isotopic signature in both bulk stable isotopes and compound specific analysis revealed input of chemosynthetic carbon, while in mobile hagfish and spider crabs, chemosynthetic carbon was only obvious *via* compound specific analysis. Based on these findings, we hence consider our chemosynthesis-based carbon-estimates conservative, and it is possible that we undervalue the input of chemosynthesis-based carbon sources to benthos. There have been observations of larger aggregations of highly mobile and vagrant taxa such as shrimps and sea-spiders in microbial mats and tufts of chemosymbiotic *Oligobrachia* worms at Arctic seeps (Sen et al., 2018a; Sen et al., 2019; Åström et al., 2019), nonetheless, whether they use the mats and tufts for feeding, hiding or as substrate still remains unanswered.

Presently, natural seepage of methane is recognized from widespread areas across the circum-Arctic (Stranne et al., 2016; Åström et al., 2020; Cramm et al., 2021) and it is predicted that

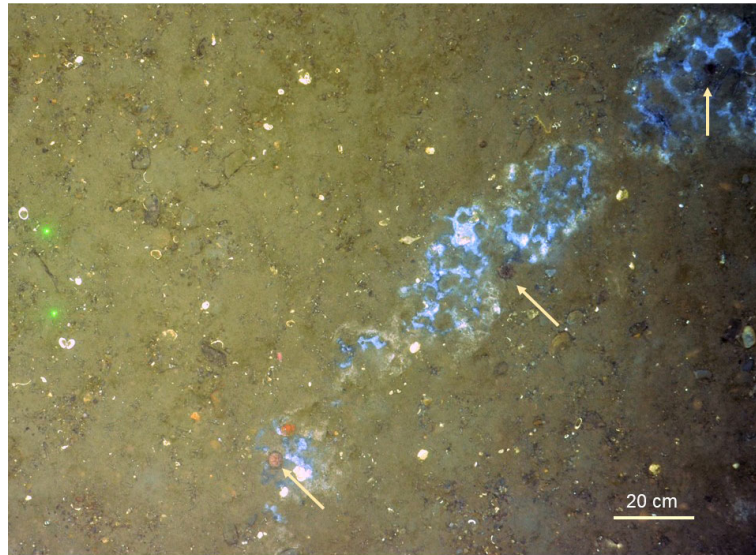


FIGURE 7

Seep site at the shallow western Svalbard margin (water depth = 85 m). Whitish/bluish microbial mats are visible at the seabed surface. It was noted that sea urchins (*Strongylocentrotus* sp., pointed out with arrows) concomitantly occurred within, or in association to, the microbial mats.

the Arctic shelves and margins holds vast amounts of gas and gas hydrates that (can) emerge from the seabed as a consequence of decreasing hydrostatic pressure from glacial periods (Solheim and Elverhøi, 1993; Wallmann et al., 2018; Shakhova et al., 2019). With such large potential of ongoing and future release of seep-hydrocarbons in the Arctic, we suggest that this carbon source likely is and will be exploited by certain background taxa. The extent thus, to which chemosynthesis-based carbon is utilized, surely varies locally depending on connectivity and intensity of pelagic-benthic coupling (Sahling et al., 2003; Vedenin et al., 2020; this study) (Figure 8). Arctic seep habitats may act as attractive zones for a broad range of background organisms as they receive input from both photosynthetic and chemosynthetic resources and a seep-stimulated upwelling would further increase the water-column productivity and generate an enhanced transport of food resources to the seabed (Pohlman et al., 2017; Ofstad et al., 2020; Sert et al., 2020). The broad range of carbon isotopic values within species seen in our study is indeed consistent with Ashford et al. (2021) who discuss a possible ‘chemotone’, the zone between an active seepage area and a background habitat where specific faunal assemblages are shaped by a mixture in food availability. Furthermore, Ashford et al. (2021) estimate that in certain areas, such a ‘chemotone’ may extend 200 m or even further away from an active seepage-area). Similarly, Levin et al. (2016) introduced the term ‘sphere of influence’ where seeps and other chemosymbiotic habitats provide a spillover effect of multiple ecosystem functions, such as nutrition and connectivity to benthic and planktonic

heterotrophic background taxa inhabiting the vicinity of seep-areas.

## Closing remarks

In view of a warming Arctic, large environmental changes are expected as well as shifts in marine carbon cycling dynamics as a result of changes in the interplay between primary surface production and ice algae (Bluhm et al., 2020; Wassmann et al., 2020). Species recognized from southern and lower latitudes appear in the Arctic region, which may cause a “borealization” of Arctic communities (Fossheim et al., 2015; Ingvaldsen et al., 2021; Snoeijs-Leijonmalm et al., 2022). One condition that determines if such new-coming species have the potential to establish viable populations in the Arctic will be the acquisition of available food resources. Reduction in sea-ice conditions and increased run-off from land, leading to potentially new patterns in upwelling and nutrient cycling will likely shift the baselines of carbon sources (McGovern et al., 2020; Wassmann et al., 2020). During such conditions, seep habitats may attract certain types of organisms as they can offer a wide niche heterogeneity and support communities with alternative carbon sources.

In this study, we have demonstrated that chemosynthesis-based carbon originating from cold seeps is used as an additional energy source in non-chemosynthetic benthic taxa, while the majority of the investigated taxa relied on sources with photosynthetic origin. This result is not surprising given that the study region is (seasonally) highly productive and

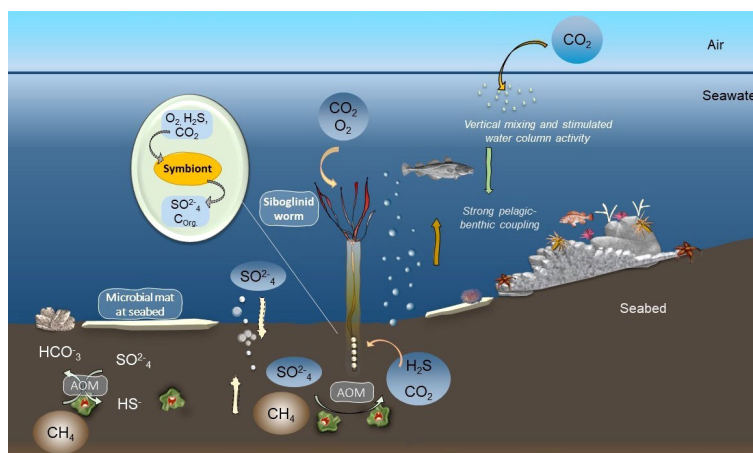


**FIGURE 8**  
Schematic illustration of anaerobic oxidation of methane (AOM) and sulfate reduction processes in the sediment (illustrated as green and red consortia) that can make chemosynthetic carbon sources available for chemosymbiotic fauna and other organisms via trophic interactions or symbiotic relationships (illustrated via the outcrop). Microbial mats can form directly on the seabed or on other surfaces (left) which allow microbial grazers to directly feed upon mats. Siboglinid worms (*Oligobranchia* sp.) from the Barents Sea can harbor thiotrophic endosymbionts (Sen et al., 2018b) that support the worms' energetic needs (middle). Through the uptake of H<sub>2</sub>S, CO<sub>2</sub> and O<sub>2</sub>, the symbionts provide organic carbon and sulfate to their host. A seep-mediated upwelling (brown arrow) may support locally enhanced surface primary-production (green dots) that subsequently settles out (green arrow), as a whole forming a tight pelagic-benthic coupling at shallow seeps. Illustration modified after Hilário et al. (2011).

characterized by relatively tight pelagic-benthic coupling. Furthermore, our results highlight the difference in use of chemosynthesis-based carbon between shallow and deeper seeps at these productive shelves, where we suggest that chemosynthesis-based carbon plays an increasingly larger role with increasing depth. We also point out that far more taxa (besides the chemosymbiotic siboglinids) can exploit these hydrocarbon-rich habitats, where some derive significant portions of their energy demand from chemosynthesis-based carbon. As the number of discovered and investigated cold seeps in the Arctic increases (Shakhova et al., 2019; Cramm et al., 2021), it is likely that the utilization of chemosynthesis-based carbon in 'background' taxa is much more prevalent than previously known (e.g. Morganti et al., 2022).

## Data availability statement

The original contributions presented in the study are included in the article/Supplementary Material. Further inquiries can be directed to the corresponding author.

## Author contributions

CRedit authorship contribution statement

EÅ: Conceptualization, Investigation, Data analysis, Writing – original draft, Writing review & editing, Visualization.

Funding acquisition. BB: Conceptualization Methodology, Investigation, Writing review & editing, Funding acquisition. TR: Methodology Investigation, Writing review & editing, Visualization. All authors contributed to the article and approved the submitted version.

## Funding

EÅ is a post-doctoral scholar funded by VISTA – a basic research program in collaboration with the Norwegian Academy of Science and Letters and Equinor (#6172). This work has partially been supported by the Research Council of Norway through the project The Nansen Legacy funding scheme, grant # 276 730. The scientific cruise in July 2018 with R/V Helmer Hanssen received support from the Research Council of Norway through its Centers of Excellence funding scheme, grant # 223 259.

## Acknowledgments

We would like to thank the chief-scientists, crew and fellow scientists onboard the R/V Helmer Hanssen cruises (CAGE 14\_1, 14\_3, 15\_2, 16\_5 18\_3 and ARCEX/AMGG2018) and R/V Kronprins Haakon (Nansen Legacy JC 1-2), for support during our sampling efforts. We are grateful to W. Hagopian at Centre for Earth Evolution and

Dynamics (UiO) for the work with isotope analyses. We would also like to thank J.S. Laberg (UiT) for cruise opportunities with ARCEX in 2018 and M. Carroll, A. Ziegler, P. Renaud and J. Pohlman for insightful discussions in the development of this work. We are thankful to the Nansen Legacy project for scientific support and network in this project.

## Conflict of interest

The authors declare that the research was conducted in the absence of any commercial or financial relationships that could be construed as a potential conflict of interest.

## References

- Ambrose, W. G. J., and Renaud, P. E. (1995). Benthic response to water column productivity patterns: Evidence for benthic-pelagic coupling in the northeast water polynya. *J. Geophys. Res. Ocean.* 100, 4411–4421. doi: 10.1029/94JC01982
- Ashford, O. S., Guan, S., Capone, D., Rigney, K., Rowley, K., Orphan, V., et al. (2021). A chemosynthetic ecotone–“chemotone”—in the sediments surrounding deep-sea methane seeps. *Limnol. Oceanogr.* 66, 1687–1702. doi: 10.1002/lno.11713
- Åström, E., Carroll, M., Ambrose, W., and Carroll, J. (2016). Arctic Cold seeps in marine methane hydrate environments: impacts on shelf macrobenthic community structure offshore Svalbard. *Mar. Ecol. Prog. Ser.* 552, 1–18. doi: 10.3354/meps11773
- Åström, E. K. L., Carroll, M. L., Ambrose, W. G., Sen, A., Silyakova, A., and Carroll, J. (2018). Methane cold seeps as biological oases in the high-Arctic deep sea. *Limnol. Oceanogr.* 63, S209–S231. doi: 10.1002/lno.10732
- Åström, E. K. L., Carroll, M., Sen, A., Niemann, H., Ambrose, W. G., Lehmann, M. F., et al. (2019). Chemosynthesis influences food web and community structure in high-Arctic benthos. *Mar. Ecol. Prog. Ser.* 629, 19–42. doi: 10.3354/meps13101
- Åström, E. K. L., Sen, A., Carroll, M. L., and Carroll, J. (2020). Cold seeps in a warming Arctic: Insights for benthic ecology. *Front. Mar. Sci.* 7. doi: 10.3389/fmars.2020.00244
- Bell, L. E., Bluhm, B. A., and Iken, K. (2016). Influence of terrestrial organic matter in marine food webs of the Beaufort Sea shelf and slope. *Mar. Ecol. Prog. Ser.* 550, 1–24. doi: 10.3354/meps11725
- Bernardino, A. F., Levin, L. A., Thurber, A. R., and Smith, C. R. (2012). Comparative composition, diversity and trophic ecology of sediment macrofauna at vents, seeps and organic falls. *PLoS One* 7, 1–17. doi: 10.1371/journal.pone.0033515
- Bluhm, B. A., Janout, M. A., Danielson, S. L., Ellingsen, I., Gavrilov, M., Grebmeier, J. M., et al. (2020). The pan-Arctic continental slope: Sharp gradients of physical processes affect pelagic and benthic ecosystems. *Front. Mar. Sci.* 7. doi: 10.3389/fmars.2020.544386
- Bluhm, B. A., Piepenburg, D., and von Juterzenka, K. (1998). Distribution, standing stock, growth, mortality and production of *Strongylocentrotus pallidus* (Echinodermata: Echinoidea) in the northern Barents Sea. *Pol. Biol.* 20, 325–334. doi: 10.1007/s003000050310
- Blumenberg, M., Lutz, R., Schlömer, S., Krüger, M., Scheeder, G., Berglar, K., et al. (2016). Hydrocarbons from near-surface sediments of the Barents Sea north of Svalbard – indication of subsurface hydrocarbon generation? *Mar. Pet. Geol.* 76, 432–443. doi: 10.1016/j.marpetgeo.2016.05.031
- Boetius, A., Albrecht, S., Bakker, K., Bienhold, C., Felden, J., Fernandez-Mendez, M., et al. (2013). Export of algal biomass from the melting Arctic Sea ice. *Science* 339, 1430–1432. doi: 10.1126/science.1231346
- Boetius, A., and Suess, E. (2004). Hydrate ridge: A natural laboratory for the study of microbial life fueled by methane from near-surface gas hydrates. *Chem. Geol.* 205, 291–310. doi: 10.1016/j.chemgeo.2003.12.034
- Childress, J. J., Fisher, C. R., Brooks, J. M., Kennicutt, M. C., Bidigare, R., and Anderson, A. E. (1986). A methanotrophic marine molluscan (Bivalvia, mytilidae) symbiosis: Mussels fueled by gas. *Science* 233, 1306–1308. doi: 10.1126/science.233.4770.1306
- Cramm, M. A., Neves, B., de, M., Manning, C. C. M., Oldenburg, T. B. P., Archambault, P., et al. (2021). Characterization of marine microbial communities around an Arctic seabed hydrocarbon seep at Scott inlet, Baffin Bay. *Sci. Tot. Environ.* 762, 143961. doi: 10.1016/j.scitotenv.2020.143961
- Decker, C., and Olu, K. (2012). Habitat heterogeneity influences cold-seep macrofaunal communities within and among seeps along the Norwegian margin. part 1: Macrofaunal community structure. *Mar. Ecol. Prog. Ser.* 445, 1–15. doi: 10.1111/j.1439-0485.2011.00503.x
- Domack, E., Ishman, S., Leventer, A., Sylva, S., Willmott, V., and Huber, B. (2005). A chemotrophic ecosystem found beneath Antarctic ice shelf. *Eos. Trans. Am. Geophys. Union.* 86, 269–272. doi: 10.1029/2005EO290001
- Dunlop, K. M., Jones, D. O. B., and Sweetman, A. K. (2018). Scavenging processes on jellyfish carcasses across a fjord depth gradient. *Limnol. Oceanogr.* 63, 1146–1155. doi: 10.1002/lno.10760
- Feng, D., Pohlman, J. W., Peckmann, J., Sun, Y., Hu, Y., Roberts, H. H., et al. (2021). Contribution of deep-sourced carbon from hydrocarbon seeps to sedimentary organic carbon: Evidence from radiocarbon and stable isotope geochemistry. *Chem. Geol.* 585, 1–8. doi: 10.1016/j.chemgeo.2021.120572
- Ferré, B., Jansson, P. G., Moser, M., Serov, P., Portnov, A., Graves, C. A., et al. (2020). Reduced methane seepage from Arctic sediments during cold bottom-water conditions. *Nat. Geosci.* 13, 144–8. doi: 10.1038/s41561-019-0515-3
- Fossheim, M., Primicerio, R., Johannesen, E., Ingvaldsen, R. B., Aschan, M. M., and Dolgov, A. V. (2015). Recent warming leads to a rapid borealization of fish communities in the Arctic. *Nat. Clim. Change* 5, 673–677. doi: 10.1038/nclimate2647
- Gebruk, A. V., Krylova, E. M., Lein, A. Y., Vinogradov, G. M., Anderson, E., Pimenov, N. V., et al. (2003). Methane seep community of the håkon mosby mud volcano (the Norwegian sea): composition and trophic aspects. *Sarsia* 88, 394–403. doi: 10.1080/00364820310003190
- Geissler, W. H., Gebhardt, A. C., Gross, F., Wollenburg, J., Jensen, L., Schmidt-Aursch, M. C., et al. (2016). Arctic Megaslide at presumed rest. *Sci. Rep.* 6, 1–8. doi: 10.1038/srep38529
- Georgieva, M. N., Wiklund, H., Bell, J. B., Eilertsen, M. H., Mills, R. A., Little, C. T. S., et al. (2015). A chemosynthetic weed: the tubeworm *Sclerolinum contortum* is a bipolar, cosmopolitan species. *BMC Evol. Biol.* 15, 280. doi: 10.1186/s12862-015-0559-y
- Graf, G. (1989). Benthic-pelagic coupling in a deep-sea benthic community. *Nature* 341, 437–439. doi: 10.1038/341437a0
- Grebmeier, J. M., and Barry, J. P. (1991). The influence of oceanographic processes on pelagic-benthic coupling in polar regions: a benthic perspective. *J. Mar. Syst.* 2, 495–518. doi: 10.1016/0924-7963(91)90049-Z

## Publisher's note

All claims expressed in this article are solely those of the authors and do not necessarily represent those of their affiliated organizations, or those of the publisher, the editors and the reviewers. Any product that may be evaluated in this article, or claim that may be made by its manufacturer, is not guaranteed or endorsed by the publisher.

## Supplementary material

The Supplementary Material for this article can be found online at: <https://www.frontiersin.org/articles/10.3389/fmars.2022.910558/full#supplementary-material>

- Hegseth, E. N., and Quillfeldt, C.V. (2022). The Sub-ice algal communities of the barents Sea pack ice: Temporal and spatial distribution of biomass and species. *J. Mar. Sci. Eng.* 10, 164. doi: 10.3390/jmse10020164.
- Higgs, N. D., Newton, J., and Attrill, M. J. (2016). Caribbean Spiny lobster fishery is underpinned by trophic subsidies from chemosynthetic primary production. *Curr. Biol.* 26, 3393–3398. doi: 10.1016/j.cub.2016.10.034
- Hilário, A., Capa, M., Dahlgren, T. G., Halanych, K. M., Little, C. T. S., Thornhill, D. J., et al. (2011). New perspectives on the ecology and evolution of siboglinid tubeworms. *PLoS One* 6, 1–14. doi: 10.1371/journal.pone.0016309
- Hobson, K., and Welch, H. (1992). Determination of trophic relationships within a high Arctic marine food web using  $\delta^{13}\text{C}$  and  $\delta^{15}\text{N}$  analysis. *Mar. Ecol. Prog. Ser.* 84, 9–18. doi: 10.3354/meps084009
- Holm-Hansen, O., Lorenzen, C., Holmes, R., and Strickland, J. (1965). Fluorometric determination of chlorophyll. *J. du Cons. Cons. Perm. Int. pour l'Explor. la Mer.* 30, 3–15. doi: 10.1093/icesjms/30.1.3
- Hügler, M., and Sievert, S. M. (2011). Beyond the Calvin cycle: Autotrophic carbon fixation in the ocean. *Ann. Rev. Mar. Sci.* 3, 261–289. doi: 10.1146/annurev-marine-120709-142712
- Ingvaldsen, R. B., Assmann, K. M., Primicerio, R., Fossheim, M., Polyakov, I. V., and Dolgov, A. V. (2021). Physical manifestations and ecological implications of Arctic atlantification. *Nat. Rev. Earth Environ.* 2, 874–889. doi: 10.1038/s43017-021-00228-x
- Jackson, A. L., Inger, R., Parnell, A. C., and Bearhop, S. (2011). Comparing isotopic niche widths among and within communities: SIBER - stable isotope Bayesian ellipses in R. *J. Anim. Ecol.* 80, 595–602. doi: 10.1111/j.1365-2656.2011.01806.x
- Kaufman, M. R., Gradinger, R. R., Bluhm, B. A., and O'Brien, D. M. (2008). Using stable isotopes to assess carbon and nitrogen turnover in the Arctic sympagic amphipod *Onisimus litoralis*. *Oecologia* 158, 11–22. doi: 10.1007/s00442-008-1122-y
- Kjesbu, O. S., Bogstad, B., Devine, J. A., Gjosæter, H., Howell, D., Ingvaldsen, R. B., et al. (2014). Synergies between climate and nitrogen management for Atlantic cod fisheries at high latitudes. *Proc. Natl. Acad. Sci.* 111, 3478 LP – 3483. doi: 10.1073/pnas.1316342111
- Layman, C. A., Arrington, D. A., Montaña, C. G., and Post, D. M. (2007). Can stable isotope ratios provide for community-wide measures of trophic structure? *Ecology* 88, 42–48. doi: 10.1890/0012-9658
- Levin, L. A., Baco, A. R., Bowden, D., Colaço, A., Cordes, E., Cunha, M. R., et al. (2016). Hydrothermal vents and methane seeps: Rethinking the sphere of influence. *Front. Mar. Sci.* 3. doi: 10.3389/fmars.2016.00072
- Levin, L. A., and Michener, R. H. (2002). Isotopic evidence for chemosynthesis-based nutrition of macrobenthos: The lightness of being at pacific methane seeps. *Limnol. Oceanogr.* 47, 1336–1345. doi: 10.4319/lo.2002.47.5.1336
- Loeng, H. (1991). Features of the physical oceanographic conditions of the barents Sea. *Pol. Res.* 10, 5–18. doi: 10.1111/j.1751-8369.1991.tb00630.x
- MacAvoy, S. E., Macko, S. A., and Carney, R. S. (2003). Links between chemosynthetic production and mobile predators on the Louisiana continental slope: stable carbon isotopes of specific fatty acids. *Chem. Geol.* 201, 229–237. doi: 10.1016/S0009-2541(03)00204-3
- Mau, S., Römer, M., Torres, M. E., Bussmann, I., Pape, T., Damm, E., et al. (2017). Widespread methane seepage along the continental margin off Svalbard from bjørnøya to kongsfjorden. *Sci. Rep.* 7, 42997. doi: 10.1038/srep42997
- McGovern, M., Poste, A. E., Oug, E., Renaud, P. E., and Trannum, H. C. (2020). Riverine impacts on benthic biodiversity and functional traits: A comparison of two sub-Arctic fjords. *Estuar. Coast. Shelf. Sci.* 240, 106774. doi: 10.1016/j.ecss.2020.106774
- McMahon, K. W., Ambrose, W. G. J., Johnson, B. J., Sun, M.-Y., Lopez, G. R., Clough, L. M., et al. (2006). Benthic community responses to ice algae and phytoplankton in ny alesund, Svalbard. *Mar. Ecol. Prog. Ser.* 310, 1–14. doi: 10.3354/meps310001
- McTigue, N. D., and Dunton, K. H. (2017). Trophodynamics of the Hanna shoal ecosystem (Chukchi Sea, Alaska): Connecting multiple end-members to a rich food web. *Deep. Res. Part II Top. Stud. Oceanogr.* 144, 175–189. doi: 10.1016/j.dsr2.2017.08.010
- Morganti, T. M., Slaby, B. M., de Kluijver, A., Busch, K., Hentschel, U., Middelburg, J. J., et al. (2022). Giant sponge grounds of central Arctic seamounts are associated with extinct seep life. *Nat. Commun.* 13, 638. doi: 10.1038/s41467-022-28129-7
- Niemann, H., Linke, P., Knittel, K., MacPherson, E., Boetius, A., Brückmann, W., et al. (2013). Methane-carbon flow into the benthic food web at cold seeps – a case study from the Costa Rica subduction zone. *PLoS One* 8, e74894. doi: 10.1371/journal.pone.0074894
- Ofstad, S., Meiland, J., Zamelczyk, K., Chierici, M., Fransson, A., Gründger, F., et al. (2020). Development, productivity, and seasonality of living planktonic foraminiferal faunas and limacina helicina in an area of intense methane seepage in the barents Sea. *J. Geophys. Res. Biogeosci.* 125, 1–24. doi: 10.1029/2019JG005387
- Oksanen, J., Blanchet, F. G., Friendly, M., Kindt, R., Legendre, P., McGlenn, D., et al. (2019). Vegan: Community ecology package. *R. Package Version.* 2.5–6, 2019.
- Onarheim, I. H., and Årthun, M. (2017). Toward an ice-free barents Sea. *Geophys. Res. Lett.* 44, 8387–8395. doi: 10.1002/2017GL074304
- Pfannkuche, O., and Thiel, H. (1987). Meiobenthic stocks and benthic activity on the NE-Svalbard shelf and in the nansen basin. *Pol. Biol.* 7, 253–266. doi: 10.1007/BF00443943
- Pohlman, J. W., Greinert, J., Ruppel, C., Silyakova, A., Vielstädte, L., Casso, M., et al. (2017). Enhanced CO<sub>2</sub> uptake at a shallow Arctic ocean seep field overwhelms the positive warming potential of emitted methane. *Proc. Natl. Acad. Sci.* 114, 5355–5360. doi: 10.1073/pnas.1618926114
- Portnov, A., Vadakkepuliambatta, S., Mienert, J., and Hubbard, A. (2016). Ice-sheet-driven methane storage and release in the Arctic. *Nat. Commun.* 7, 10314. doi: 10.1038/ncomms10314
- Post, D. M. (2002). Using stable isotopes to estimate trophic position: Models, methods, and assumptions. *Ecology* 83, 703–718. doi: 10.1890/0012-9658(2002)083[0703:USITET]2.0.CO;2
- Rasmussen, T. L., Laberg, J. S., Ofstad, S., Rydingen, T., Åström, E. K. L., El Bani Altuna, N., et al. (2018). Cruise report - AMGG cruise to the northern and eastern Svalbard margin on R/V helmer hanssen. <https://cage.uit.no/cruise/amgg-research-school-cruise-2018/> (assessed June 1, 2021)
- Rasmussen, T. L., Nielsen, T., Ofstad, S., Åström, E. K. L., El Bani Altuna, N., Laier, T., et al. (2018b). CAGE-18-3 cruise to the barents Sea, storfjorden trough, East Greenland ridge (Leg 1, 2) (Arctic Ocean, Vestnesa Ridge: PKF (Leg 3). available online at: <https://cage.uit.no/cruise/methane-seep-site-investigation/> (accessed June 1, 2021)
- Ravelo, A. M., Konar, B., Bluhm, B., and Iken, K. (2017). Growth and production of the brittle stars *ophiura sarsii* and *ophiocten sericeum* (Echinodermata: Ophiuroidea). *Cont. Shelf. Res.* 139, 9–20. doi: 10.1016/j.csr.2017.03.011
- Renaud, P. E., Løkken, T. S., Jørgensen, L. L., Berge, J., and Johnson, B. J. (2015). Macroalgal detritus and food-web subsidies along an Arctic fjord depth-gradient. *Front. Mar. Sci.* 2. doi: 10.3389/fmars.2015.00031
- Renaud, P., Tessmann, M., Evensen, A., and Christensen, G. (2011). Benthic food-web structure of an Arctic fjord (Kongsfjorden, Svalbard). *Mar. Biol. Res.* 7, 13–26. doi: 10.1080/17451001003671597
- Robinson, J. J., and Cavanaugh, C. M. (1995). Expression of form I and form II rubisco in chemoautotrophic symbioses: Implications for the interpretation of stable carbon isotope values. *Limnol. Oceanogr.* 40, 1496–1502. doi: 10.4319/lo.1995.40.8.1496
- Soreide, J. E., Hop, H., Carroll, M. L., Falk-Petersen, S., and Hegseth, E. N. (2006). Seasonal food web structures and sympagic–pelagic coupling in the European Arctic revealed by stable isotopes and a two-source food web model. *Prog. Oceanogr.* 71, 59–87. doi: 10.1016/j.pocan.2006.06.001
- Sahling, H., Galkin, S. V., Salyuk, A., Greinert, J., Foerstel, H., Piepenburg, D., et al. (2003). Depth-related structure and ecological significance of cold-seep communities—a case study from the Sea of Okhotsk. *Deep. Sea. Res. Part I. Oceanogr. Res. Pap.*, 50, 1391–1409. doi: 10.1016/j.dsr.2003.08.004
- Sahling, H., Römer, M., Pape, T., Bergès, B., dos Santos Fereira, C., Boelmann, J., et al. (2014). Gas emissions at the continental margin west of Svalbard: mapping, sampling, and quantification. *Biogeosciences* 11, 6029–6046. doi: 10.5194/bg-11-6029-2014
- Schubert, C. J., and Calvert, S. E. (2001). Nitrogen and carbon isotopic composition of marine and terrestrial organic matter in Arctic ocean sediments: implications for nutrient utilization and organic matter composition. *Deep. Sea. Res. Part I. Oceanogr. Res. Pap.* 48, 789–810. doi: 10.1016/S0967-0637(00)00669-8
- Seabrook, S., De Leo, F. C., and Thurber, A. R. (2019). Flipping for food: The use of a methane seep by tanner crabs (*Chionoecetes tanneri*). *Front. Mar. Sci.* 6. doi: 10.3389/fmars.2019.00043
- Sen, A., Åström, E. K. L., Hong, W.-L., Portnov, A., Waage, M., Serov, P., et al. (2018a). Geophysical and geochemical controls on the megafaunal community of a high Arctic cold seep. *Biogeosciences* 15, 4533–4559. doi: 10.5194/bg-15-4533-2018
- Sen, A., Duperron, S., Hourdez, S., Piquet, B., Léger, N., Gebruk, A., et al. (2018b). Cryptic frenulates are the dominant chemosymbiotic fauna at Arctic and high latitude Atlantic cold seeps. *PLoS One* 13, e0209273. doi: 10.1371/journal.pone.0209273
- Sen, A., Himmler, T., Hong, W. L., Chitkara, C., Lee, R. W., Ferré, B., et al. (2019). Atypical biological features of a new cold seep site on the lofoten-vesteralen continental margin (northern Norway). *Sci. Rep.* 9, 1762. doi: 10.1038/s41598-018-38070-9
- Serov, P., Vadakkepuliambatta, S., Mienert, J., Patton, H., Portnov, A., Silyakova, A., et al. (2017). Postglacial response of Arctic ocean gas hydrates to

- climatic amelioration. *Proc. Natl. Acad. Sci.* 114, 6215–6220. doi: 10.1073/pnas.1619288114
- Sert, M. F., D'Andrilli, J., Gründger, F., Niemann, H., Granskog, M. A., Pavlov, A. K., et al. (2020). Compositional differences in dissolved organic matter between Arctic cold seeps versus non-seep sites at the Svalbard continental margin and the barents Sea. *Front. Earth Sci.* 8. doi: 10.3389/feart.2020.552731
- Shakhova, N., Semiletov, I., and Chuvilin, E. (2019). Understanding the permafrost-hydrate system and associated methane releases in the East Siberian Arctic shelf. *Geosciences* 9, 251. doi: 10.3390/geosciences9060251
- Snoeijs-Leijonmalm, P., Flores, H., Sakinam, S., Hildebrandt, N., Svenson, A., Castellani, G., et al. (2022). Unexpected fish and squid in the central Arctic deep scattering layer. *Sci. Adv.* 8, eabj7536. doi: 10.1126/sciadv.abj7536
- Sokolowski, A., Szczepańska, A., Richard, P., Kędra, M., Wołowicz, M., and Węśławski, J. M. (2014). Trophic structure of the macrobenthic community of hornsund, spitsbergen, based on the determination of stable carbon and nitrogen isotopic signatures. *Pol. Biol.* 37, 1247–1260. doi: 10.1007/s00300-014-1517-7
- Solheim, A., and Elverhøi, A. (1993). Gas-related sea floor craters in the barents Sea. *Geo-Mar. Lett.* 13, 235–243. doi: 10.1007/BF01207753
- Sorokin, Y. I., and Sorokin, P. Y. (1996). Plankton and primary production in the Lena river estuary and in the south-eastern laptev Sea. *Estuar. Coast. Shelf. Sci.* 43, 399–418. doi: 10.1006/ecs.1996.0078
- Stevens, C. J., Juniper, S. K., Limén, H., Pond, D. W., Metaxas, A., and Gélinais, Y. (2015). Obligate hydrothermal vent fauna at East diamante submarine volcano (Mariana arc) exploit photosynthetic and chemosynthetic carbon sources. *Mar. Ecol. Prog. Ser.* 525, 25–39. doi: 10.3354/meps11229
- Stranne, C., O'Regan, M., Dickens, G. R., Crill, P., Miller, C., Preto, P., et al. (2016). Dynamic simulations of potential methane release from East Siberian continental slope sediments. *Geochem. Geophys. Geosyst.* 17, 872–886. doi: 10.1002/2015GC006119
- Svendsen, H., Beszczynska-Möller, A., Hagen, J. O., Lefauconnier, B., Tverberg, V., Gerland, S., et al. (2002). The physical environment of kongsfjorden-krossfjorden, an Arctic fjord system in Svalbard. *Pol. Res.* 21, 133–166. doi: 10.3402/polar.v21i1.6479
- Sweetman, A., Levin, L., Rapp, H., and Schander, C. (2013). Faunal trophic structure at hydrothermal vents on the southern mohn's ridge, Arctic ocean. *Mar. Ecol. Prog. Ser.* 473, 115–131. doi: 10.3354/meps10050
- Syvrtsen, E. E. (1991). Ice algae in the barents Sea: types of assemblages, origin, fate and role in the ice-edge phytoplankton bloom. *Pol. Res.* 10, 277–288. doi: 10.3402/polar.v10i1.6746
- Tarasov, V. G., Gebruk, A. V., Mironov, A. N., and Moskalev, L. I. (2005). Deep-sea and shallow-water hydrothermal vent communities: Two different phenomena? *Chem. Geol.* 224, 5–39. doi: 10.1016/j.chemgeo.2005.07.021
- Terwilliger, N. B. (1998). Functional adaptations of oxygen-transport proteins. *J. Exp. Biol.* 201, 1085–1098. doi: 10.1242/jeb.201.8.1085
- Toone, T. A., and Washburn, T. W. (2020). Phytodetritus, chemosynthesis, and the dark biosphere: Does depth influence trophic relationships at deep-sea Barbados seeps. *Deep. Sea. Res. Part I. Oceanogr. Res. Pap.* 165, 103367. doi: 10.1016/j.dsr.2020.103367
- Vedenin, A. A., Kokarev, V. N., Chikina, M. V., Basin, B., Galkin, S. V., and Gebruk, A. V. (2020). Fauna associated with shallow-water methane seeps in the laptev Sea. *PeerJ* 8, e9018. doi: 10.7717/peerj.9018
- Vihtakari, M. (2021). ggOceanMaps: Plot data on oceanographic maps using "ggplot2". doi: 10.5281/zenodo/4790048. (accessed June 9, 2021)
- Vismann, B. (1991). Sulfide tolerance: physiological mechanisms and ecological implications. *Ophelia* 34, 1–27. doi: 10.1080/00785326.1991.10429703
- Wallmann, K., Riedel, M., Hong, W. L., Patton, H., Hubbard, A., Pape, T., et al. (2018). Gas hydrate dissociation off Svalbard induced by isostatic rebound rather than global warming. *Nat. Commun.* 9, 83. doi: 10.1038/s41467-017-02550-9
- Wassmann, P., Carmack, E. C., Bluhm, B. A., Duarte, C. M., Berge, J., Brown, K., et al. (2020). Towards a unifying pan-arctic perspective: A conceptual modelling toolkit. *Prog. Oceanogr.* 189, 102455. doi: 10.1016/j.pocean.2020.102455
- Wassmann, P., Reigstad, M., Haug, T., Rudels, B., Carroll, M. L., Hop, H., et al. (2006). Food webs and carbon flux in the barents Sea. *Prog. Oceanogr.* 71, 232–287. doi: 10.1016/j.pocean.2006.10.003
- Weems, J., Iken, K., Gradinger, R., and Wooller, M. J. (2012). Carbon and nitrogen assimilation in the Bering Sea clams *nuculana radiata* and *macoma moesta*. *J. Exp. Mar. Bio. Ecol.* 430–431, 32–42. doi: 10.1016/j.jembe.2012.06.015
- Wei, C.-L., Rowe, G. T., Escobar-Briones, E., Boetius, A., Soltwedel, T., Caley, M. J., et al. (2011). Global patterns and predictions of seafloor biomass using random forests. *PLoS One* 5, e15323. doi: 10.1371/journal.pone.0015323
- Wiedmann, I., Ershova, E., Bluhm, B. A., Nöthig, E., Gradinger, R. R., Kosobokova, K., et al. (2020). What feeds the benthos in the Arctic basins? assembling a carbon budget for the deep Arctic ocean. *Front. Mar. Sci.* 7. doi: 10.3389/fmars.2020.00224
- WoRMS Editorial Board. (2022). *World Register of Marine Species*. Available from <https://www.marinespecies.org> at VLIZ. Accessed 2022-08-01. doi: 10.14284/170
- Zaborska, A., Carroll, J., Papucci, C., Torricelli, L., Carroll, M. L., Walkusz-Miotk, J., et al. (2008). Recent sediment accumulation rates for the Western margin of the barents Sea. *Deep. Sea. Res. Part II Top. Stud. Oceanogr.* 55, 2352–2360. doi: 10.1016/j.dsr2.2008.05.026
- Vander Zanden, M. J., and Rasmussen, J. B. (2001). Variation in  $\delta^{15}\text{N}$  and  $\delta^{13}\text{C}$  trophic fractionation: Implications for aquatic food web studies. *Limnol. Oceanogr.* 46, 2061–2066. doi: 10.4319/lo.2001.46.8.2061
- Zapata-Hernández, G., Sellanes, J., Thurber, A. R., Levin, L. A., Chazalon, F., and Linke, P. (2014). New insights on the trophic ecology of bathyal communities from the methane seep area off concepción, Chile ( $\sim 36^\circ$  s). *Mar. Ecol.* 35, 1–21. doi: 10.1111/maec.12051